ENGINEERING RESEARCH INSTITUTE
UNIVERSITY OF MICHIGAN
ANN ARBOR

METAL CUTTING WITH CONTROLLED ELECTRIC ARCS

JOSEPH DATSKO
Assistant Professor of Production Engineering

M. B. FOLKERT

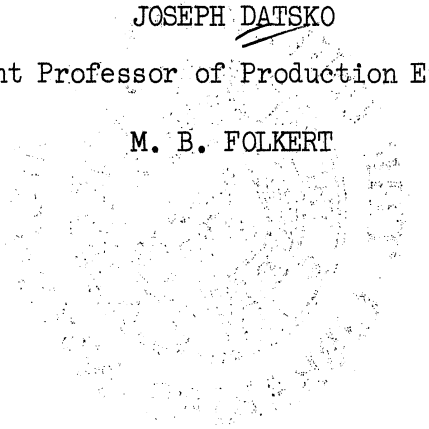

Project 2175

CLINTON MACHINE COMPANY, METALMASTER DIVISION
CLINTON, MICHIGAN

December, 1954

Erm

UMRC597

TABLE OF CONTENTS

ABSTRACT

Although it is possible to use straight dc current to drill holes by the electrospark process, it is not very practical since it produces oversized and rough holes. A resistance-capacitance type circuit gives much better results. For the most rapid drilling, capacitance of 100 to 300 microfarads with a resistance of 3 to 25 ohms should be used. However, better surface finishes are obtained with a combination of 10 microfarads and 100 ohms. Although drilling does occur without head vibrations, the best results were obtained when the head was vibrated about 200 cycles per second.

A detailed metallographic study of surfaces produced by the electrospark process showed that the mechanism of metal removal is one of thermal means, which is obvious in consideration of the microstructure changes beneath the surface. Studies of holes drilled by the method "X" process showed the same signs of transformation due to high temperatures as did the specimens drilled with the Metalmaster disintegrator.

The tests conducted with a disk-type electrode showed that the disk does wear quite rapidly, and consequently it is felt that external machining would be most feasible on the very hard, abrasive work materials such as titanium and sintered carbide.

From the wide range of tests made comparing tools sharpened by means of electrosparking to tools sharpened by diamond grinding, several interesting facts were observed. First, the reliability of the performance (that is, the amount of variation in the tool life there would be between several tools sharpened under identical conditions) of electrosparked tools is as good as that of diamond-ground tools. Secondly, in machining cast iron without a cutting fluid, the flank wear of both electrosparked and diamond-ground tools were very nearly alike. Finally, in turning SAE 1045 while using a cutting fluid, it was found that the electrosparked tool performed as well as a similar tool that was diamond-ground to a much better finish.

In the brief residual stress studies made, it was found that stresses were induced in the work material that were quite similar to the stresses induced by abrasive grinding. Since the nature of the residual stresses beneath any machined surface is of great importance to the satisfactory service of the part, it is felt that the nature and cause of these residual stresses should be the subject of any future study made on this machining process.

METAL CUTTING WITH CONTROLLED ELECTRIC ARCS

I. INTRODUCTION

This report deals exclusively with the use of a dc source for the energy dissipated in the arc. It is an extension of the previous report that explained the characteristics of the original Metalmaster disentegrator. The experimental work was carried out using 0.140-inch-diameter molybdenum and copper tubes as the electrode when drilling and a 9-inch-diameter by 1/4-inch-thick copper disc when grinding. Two types of circuits were studied, the first being a simple dc source connected directly to the vibrating electrode and the second, an R-C circuit, that is, one having a resistance in series and a capacitance in parallel with the arc.

II. DIRECTLY CONNECTED DC SOURCE

A welding generator whose open-circuit voltage and short-circuit current could be controlled was connected with its negative terminal to the head of the Metalmaster and its positive terminal to the work. The head was vibrated at a rate of 60 cycles per second. The best results with this connection were obtained with an open-circuit voltage of 15 volts and an average current of 40 amperes, and with the electrode-held negative. The time necessary to drill a hole 5/16 inch deep in cold-rolled steel was 4 minutes. The corresponding molybdenum electrode disintegration was 1/16 inch. In all cases the holes obtained with this circuit were visibly larger and rougher than those obtained with the original ac circuit.

When using this connection the arc is never extinguished but continues to burn even though the electrode is withdrawn from the work by the solenoid. This is due to the inductance of the leads and the dc source. The reason for the poor holes obtained appears to be that the arc prevents the coolant from coming in contact with the hot surfaces of the workpiece.

Tests were also run with the electrode positive and the work negative. This approximately doubled the drilling time and increased the electrode wear by a factor of four. This confirms the previous conclusion that the electrode should be negative and the work positive.

III. RESISTANCE-CAPACITANCE CIRCUIT

The need for providing a means of holding the electrode voltage down momentarily when the electrode separates from the work so that the arc may be extinguished suggested the use of a capacitor in parallel with the arc. Figure 1 shows a resistance-capacitance circuit devised for this purpose. The resistance must be included in order to limit the charging current of the condenser and control the current through the arc. The electrode was used as the negative and the work as the positive members of the circuit. The supply voltage was 110 volts dc obtained from a motor-generator set. The electrode was again held in the Metalmaster head and was vibrated at various frequencies during the tests.

The condenser performs a second function as an energy storage unit. The energy stored in the condenser is $w=1/2\ CV^2$ joules, where C is the capacitance in farads and V is the voltage across the condenser. Just before the electrode is brought in contact with the work the condenser is charged to the supply voltage. As soon as contact is made this energy is released to the electrode-work junction and instantaneously establishes a high temperature at this junction. The temperature of an arc has been determined experimentally to be approximately 11,000°F. The top half of Fig. 2 shows the voltage pattern between the workpiece and the copper electrode. The head was vibrating at a rate of 60 cycles per second. The resistance was 5 ohms and the capacity 130 microfarads. The events during one head cycle are as follows. When the electrode initially touches the work an electrical contact is established and the voltage drops to zero. The condenser has completely discharged and the circuit is again interrupted with the condenser beginning to recharge. This interruption appears to be due to the electrode bouncing back. The condenser does not recharge completely before the electrode again contacts the work with the arcing process following. The arcing, however, is intermittent with physical contact established several times before the electrode is withdrawn by the head. After the electrode is withdrawn and the arc is extinguished, the condenser charges to the supply voltage with the voltage remaining constant until the head again lowers the electrode onto the work.

The electrode current pattern is shown immediately below the voltage pattern in Fig. 2. Its magnitude is not correct due to the metering system used, but it does show when the current flows. During the arcing process, it is only when both current and voltage are present that energy is delivered to

the work surface. Thus, Fig. 2 shows that energy is delivered to the workpiece only during 1/5 of the time that the electrode is down.

Figure 3 shows the damped oscillatory current pattern obtained when the electrode actually touches the work. From it and from the voltage pattern of Fig. 1 the following equivalent circuit of Fig. 4 was obtained. The circuit elements are as follows: R is the resistance inserted to limit the charging rate of the condenser and to control the current through the arc; C is the capacitance in parallel with the arc; R_2 and L are the resistance and inductance of the leads connecting the condenser to the electrodes. L was calculated from Fig. 3 to be 4.95 microhenries and R was calculated to be 0.049 ohms. Any inductance in the series with R may be neglected. As a check, the charging time constant of the condenser, neglecting inductance, was calculated to be 0.00065 second and scaled from the oscillogram to be 0.00063 second.

The original stored energy in the condenser is dissipated very rapidly in the gap at the beginning of the arcing period and thus the current which flows during most of the period is determined by the resistor R. Fast cutting rates are thus obtained with low resistance and large condenser capacities since a low resistance allows the average current to be higher and a large condenser capacity provides large supply of stored energy. The charging time of the condenser is approximately 4 R-C seconds and sets an upper limit to the capacity value.

A. Performance Tests with R-C Circuit

Tests were made to determine whether it is necessary to vibrate the head with this circuit. It was found that a careful operator using an oscilloscope to monitor the head voltage could drill successfully without head vibrations. Figure 5 shows the time taken to drill a 1/4-inch-deep hole in cold-rolled steel for various values of resistance and capacity. Since the results depend on the skill of the operator to a great extent the remainder of the tests were carried out with the head vibrating. The results, however, do indicate that it might be possible to drill with this circuit without head vibrations if a servomechanism feed is used.

In order to study the effect of head vibration, a 400-cycle generator whose frequency could be controlled was used as the supply for the head solenoid through the rectifier. The frequency was varied between 60 and 400 cycles. The results of some typical tests for various values are shown in Fig. 6. In all cases 200 cycles was the frequency which gave minimum drilling time.

Tests were made to determine the optimum value of capacitance to be used. Figures 7 and 8 show the results of such a test made on 1/4-inch

Fig. 3. Oscillogram Showing Oscillatory Current Pattern Obtained When Electrode Makes Physical Contact With Work. Frequency of Oscillations is 6,250 Cycles per Second. Resistance is 5 ohms Capacity 130 Microfarads.

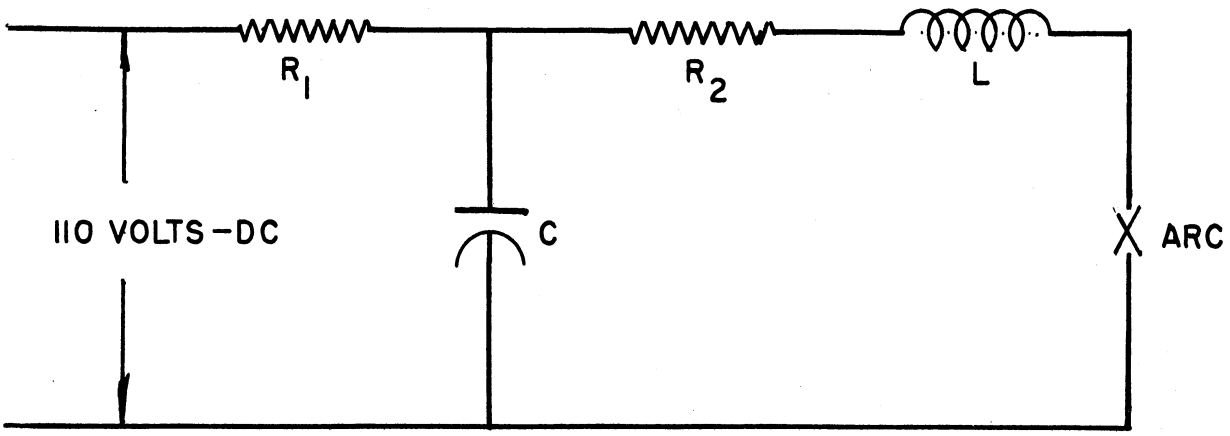

Fig. 4. Equivalent Circuit

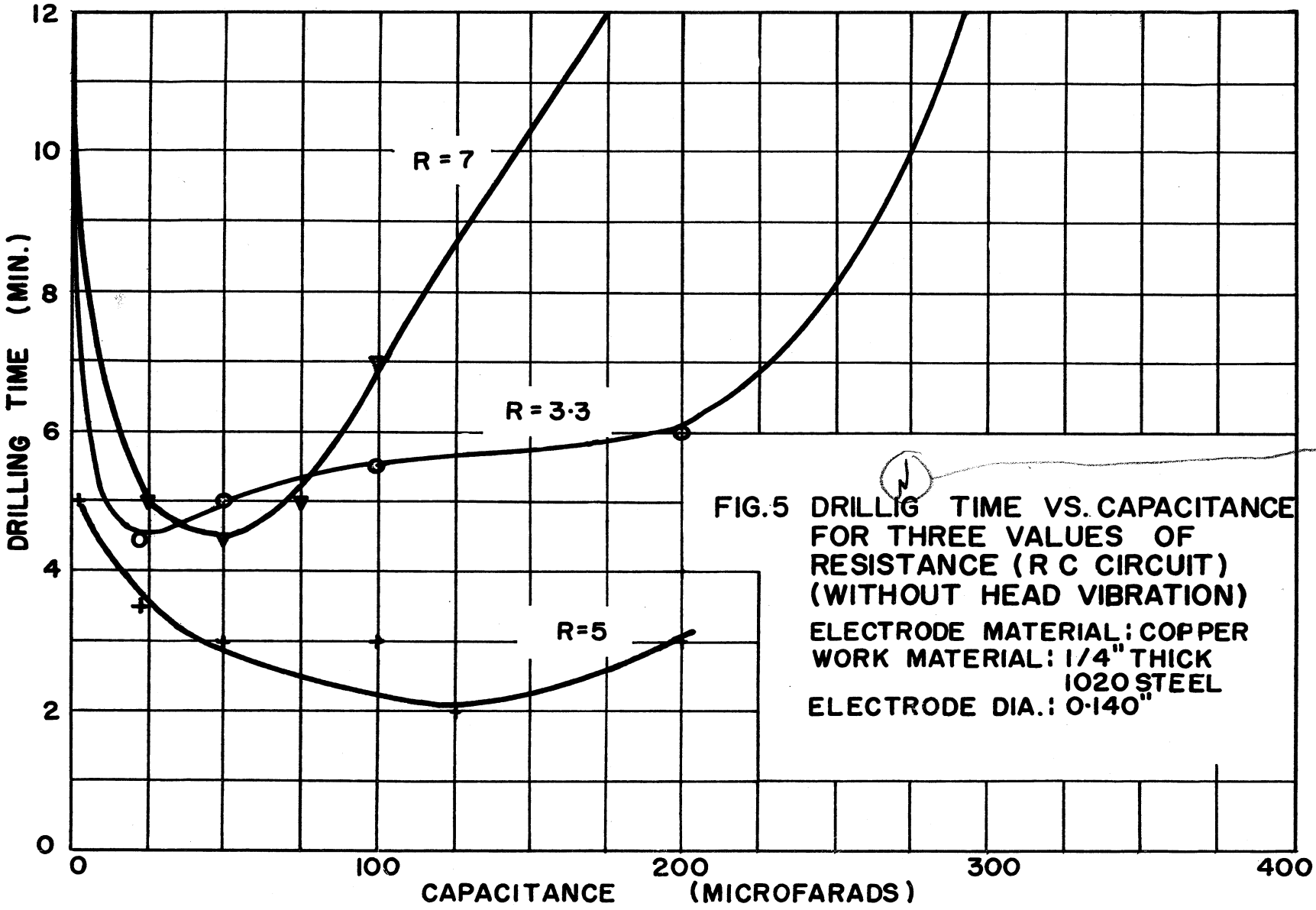

FIG.5 DRILLIG TIME VS. CAPACITANCE FOR THREE VALUES OF RESISTANCE (R C CIRCUIT) (WITHOUT HEAD VIBRATION)

ELECTRODE MATERIAL: COPPER
WORK MATERIAL: 1/4" THICK 1020 STEEL
ELECTRODE DIA.: 0·140"

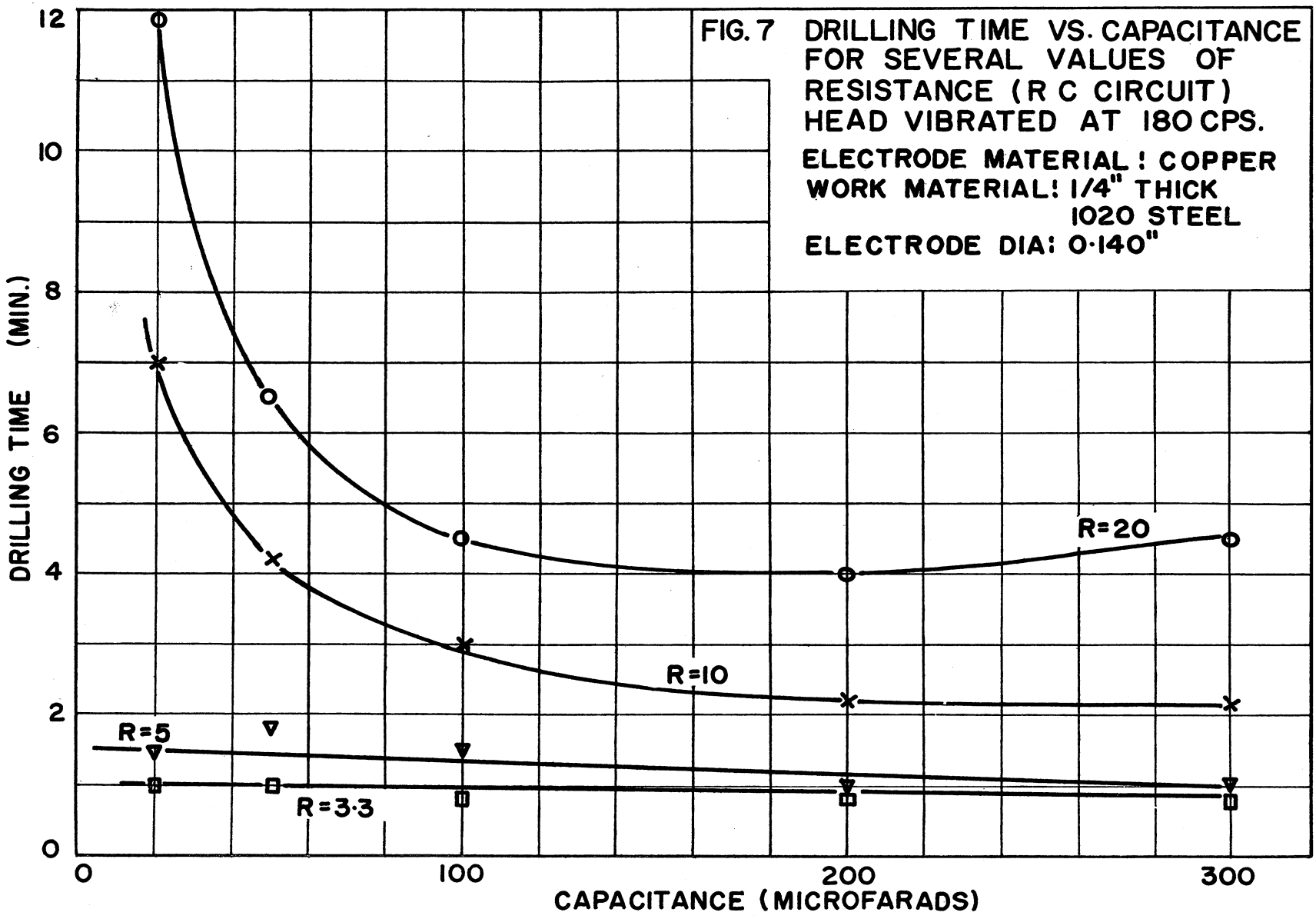
FIG. 7 DRILLING TIME VS. CAPACITANCE FOR SEVERAL VALUES OF RESISTANCE (R C CIRCUIT) HEAD VIBRATED AT 180 CPS.
ELECTRODE MATERIAL : COPPER
WORK MATERIAL: 1/4" THICK 1020 STEEL
ELECTRODE DIA: 0·140"
DRILLING TIME (MIN.)
CAPACITANCE (MICROFARADS)
0
2
4
6
8
10
12
0
100
200
300
R=20
R=10
R=5
R=3·3

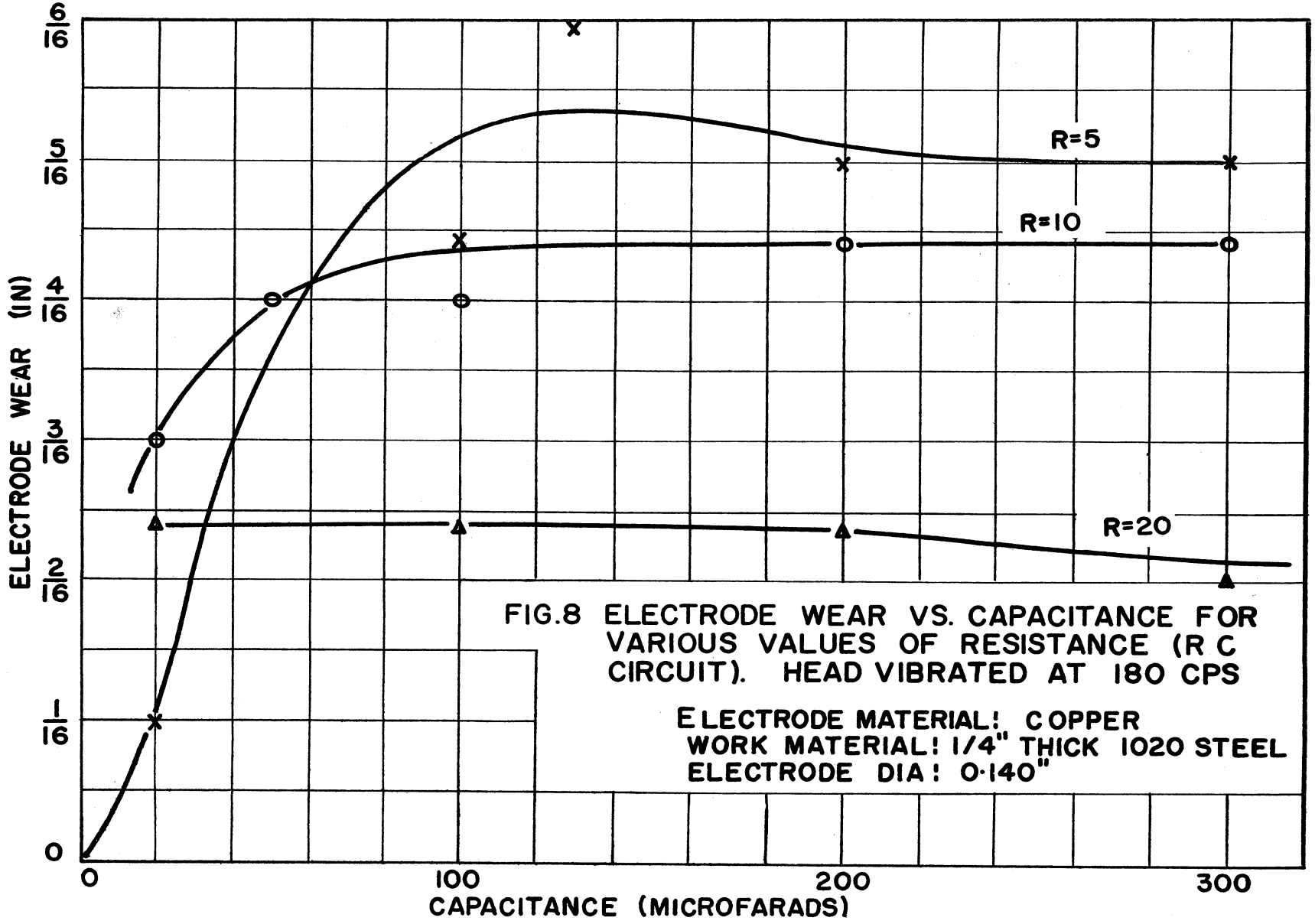

FIG.8 ELECTRODE WEAR VS. CAPACITANCE FOR VARIOUS VALUES OF RESISTANCE (R C CIRCUIT). HEAD VIBRATED AT 180 CPS

ELECTRODE MATERIAL: COPPER
WORK MATERIAL: 1/4" THICK 1020 STEEL
ELECTRODE DIA: 0·140"

AISI 1020 steel using copper electrodes with the head vibrating at a rate of 180 cycles per second. The tests show capacities ranging from 100 to 300 microfarads to be suitable.

B. Drilling of Carbon Steels

This series of tests was conducted on 1/4-inch-thick blocks of low-carbon steel, hardened tool steel, and high-speed steel, using both copper and molybdenum electrodes. As seen in Table I, increasing the hardness of the steel produced no increase in either the cutting time or the electrode wear. With resistance of 5 ohms the hole quality is poorer than at 10 or 20 ohms, although the cutting time is less, and therefore a compromise must be reached between cutting rate and hole qualities. Satisfactory results are achieved by using a resistance of 10 ohms and a capacity of 100 to 300 microfarads; where very accurate and smooth work is required, 20 ohms or more should be used at a vibration frequency of 200 cps.

It was observed that with one can of fresh coolant and a resistance of 10 or 20 ohms and a capacitance of 100 to 300 microfarads, as the frequency of head vibration was increased, material would plate on the electrode. The electrode plus the plated material would then act as an electrode and the end result was that the hole would get larger as it went deeper. This effect is at its worst with the softer metals, such as AISI 1020 and tool steel. With high-speed steel it is practically negligible and with such substances as cast, nonferrous metals, it was practically nonexistent. The photograph in Fig. 9 shows this effect in tool steel at frequencies of 60, 180, and 300 cycles. It was impossible to repeat these results with a second batch of cutting fluid and no further study of this was made.

C. Drilling of Stainless Steel

Tests were made in 1/4-inch-thick blocks of stainless steel similar to those of the previously discussed tests, and runs were made using both the molybdenum and copper electrodes. Slower cutting rates, as shown in Table I, and poorer holes were encountered with the copper electrodes in the stainless steel as compared to the carbon steel. The copper electrodes had a tendency to become tapered as the hole became deeper and this in turn produced tapered holes. This effect was at its worst with high-resistance values (10 and 20 ohms). No taper was observed with the molybdenum electrodes.

D. Drilling of Sintered Tungsten Carbide

The tests were repeated with blocks of tungsten carbide using both types of electrodes (molybdenum and copper). It was observed that the cutting

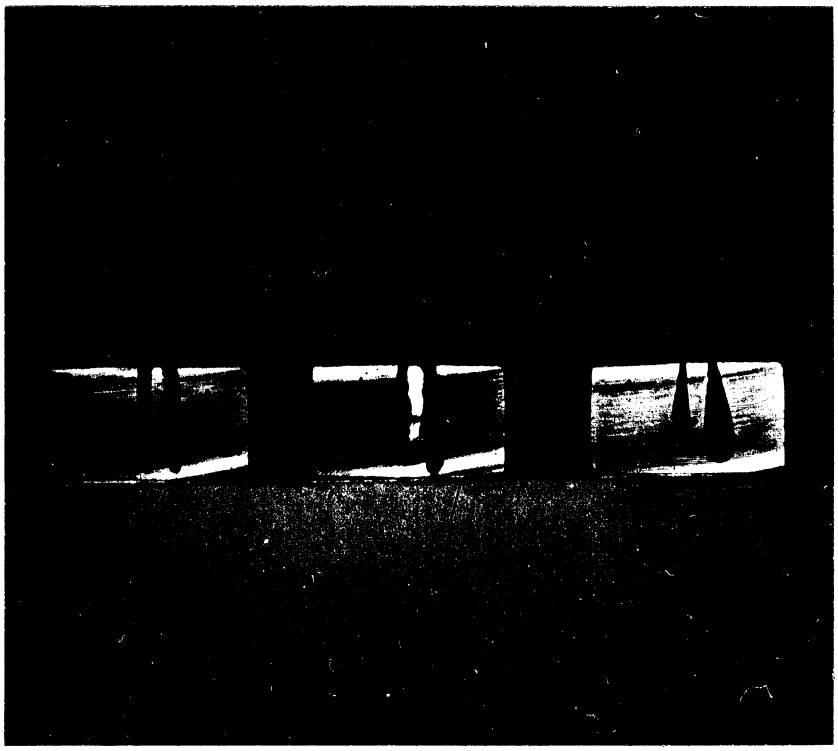

Fig. 9. Photograph of Holes in Sectioned Blocks of Tool Steel Showing Evidence of Electrode Build-up. Resistance is 10 ohms and capacity is 100 microfarads. Molybdenum electrode was used. Head vibration rate for blocks from left to right is 60, 180, and 300 cycles per second, respectively.

TABLE I

DRILLING TIME AND ELECTRODE WEAR FOR REPRESENTATIVE MATERIALS

HEAD VIBRATION: 300 CPS
HOLE DEPTH: 1/4"
CAPACITANCE – MICROFARADS
RESISTANCE – OHMS

TIME (MIN.) / ELECTODE WEAR (1/16")

MOLY ELECTRODE

R \ C	300	200	100	50	20	0
33	1/2 + / 3	1/2 + / 2	3/4 / 2	3/4 / 1	1 / 1/2	1 / 1/2
5	1 / 2	1 / 2	1+ / 2	1 1/4 + / 1 1/2	1 3/4 / 1	2 / 1/2
10	3 / 1–	2 1/4 / 1 1/2	2 1/2 / 1 1/2	2 3/4 / 1 1/2	4 1/2 / 1 1/2	6 3/4 / NEG.
20	8 1/4 / 1/2	6 1/2 / 1	5 1/4 / 1	5 1/2 / 1	9 1/4 / 1	

COPPER ELECTRODE

R \ C	300	200	100	50	20	0
33	3/4 / 7	3/4 / 2 1/2	3/4 / 1 1/2	3/4 / 1	3/4 / NEG.	3/4 / NEG.
5	1 / 2 1/2	1 / 2	1+ / 2	1 1/4 + / 1 1/2	1 1/2 / 1/2	1 3/4 / NEG.
10	2 1/4 / 2	2 / 2	2 / 2	2 3/4 / 2	5 / 1 1/2	8 1/2 / NEG.
20	5 3/4 / 1	4 1/2 / 1	3 3/4 / 1	4 1/4 / 1		

LOW CARBON STEEL

MOLY ELECTRODE

R \ C	300	200	100	50	20	0
33	1/2 / 2	1/2 / 1 1/2	3/4 / 1	1 / 1	1 1/8 / NEG.	1 1/4 / NEG.
5	3/4 / 1	3/4 / 1 1/2	1 / 1 1/2	1 1/4 / 1	1 3/4 / 1/2	2 / NEG.
10	2 / 1	2 / 1	2 / 1	2 1/2 / 1	3 3/4 / 1	8 / NEG.
20	6 / 1	4 / 1	4 / 1	4 1/4 / 1	6 3/4 / 1	15 / NEG.

COPPER ELECTRODE

R \ C	300	200	100	50	20	0
33	1/2 / 2	1/2 / 2	1/2 + / 1 1/2	3/4 / 1	3/4 / NEG.	3/4 / NEG.
5	3/4 / 2	3/4 / 2	1 / 1 1/2	1 / 1	1 1/4 / 1/2	1 1/4 / NEG.
10	2 1/2 / 1 1/2	2 1/4 / 1 1/2	1 3/4 / 1 1/2	2 1/4 / 1 1/2	4 / 1–	6 1/4 / NEG.
20	6 / 1/2	5 1/2 / 1	4 / 1	4 3/4 / 1/2		

HIGH SPEED STEEL

COPPER ELECTRODE

R \ C	300	200	100	50	20	0
33	1 / 3 1/2	1 / 1 1/2	1 / 1 1/2	1 / 1	1 / 1/2	1 / 1/2
5	1 1/4 / 1+	1 / 2	1 / 1	1 1/2 / 1 1/2	1 3/4 / NEG.	2 1/4 / NEG.
10	2 3/4 / 1+	2 1/2 / 1	2 1/4 / 1	2 1/2 / 1/2	3 1/2 / 1	13 / NEG
20	20 / NEG.	6 3/4 / 1/2	5 / 1/2	4 1/2 / 1	6 1/4 / 1	

HARDENED TOOL STEEL

TABLE I CONT'D

C / R	300	200	100	50	20	0
3·3	1/2 / 2	1/2 / 2	3/4 / 1+	1 1/4 / 1	1 1/4 / —	1 1/4 / NEG.
5	1/2 / 2 1/2	3/4 / 2 1/2	1 / 2	1 1/4 / 1 1/2	2 1/4 / 1/2	2 1/2 / NEG.
10	1 1/2 / 1 1/2	1 3/4 / 2	1 1/2 / 2	2 1/4 / 2	5 / 2	14 1/2 / NEG.
20	5 /	3 3/4 / 1	2 3/4 / 1	3 1/2 / 2	5 3/4 / 1	

MOLY ELECTRODE

C / R	300	200	100	50	20	0
3·3	3/4 / 3	1 / 2	1 / 2	1 / 2	1 3/4 / 1	1 3/4 / 1
5	1 /	1 /	1 1/4 /	1 1/2 /	1 1/2 /	1 3/4 /
10	1 3/4 / 2	2 1/4 / 2	2 1/2 / 2	3 / 2	5 / 1	11 1/2 / NEG.
20	14 1/2 / 1	9 / 1 1/2	7 1/2 / 1 1/2	5 / 2	/	/

COPPER ELECTRODE

STAINLESS STEEL

C / R	300	200	100	50	20	0
3·3	2 1/2 / 5	2 1/4 / 5	2 1/4 / 2 1/2	2 3/4 / 2	/	/
5	3 3/4 / 4	3 1/4 / 3	4 1/2 / 2	4 1/2 / 2	/	/
10	10 / 3	5 / 6	5 3/4 / 6	7 3/4 / 4	/	/
20	13 3/4 / 3	12 1/4 / 3	13 3/4 / 5	11 1/2 / 5	/	/

MOLY ELECTRODE

C / R	300	200	100	50	20	0
3·3	3 1/4 / 6 1/2	4 1/2 / 4	3 / 2	3 3/4 / NEG.	/	/
5	5 1/2 / 3	4 1/2 / 3	7 / 2 1/2	/	/	/
10	8 / NEG.	8 / NEG.	7 3/4 / 2 1/2	8 / NEG.	/	/
20	15 / NEG	13 1/4 / 1/2	10 3/4 / 1/2	10 1/4 / 1/2	/	/

COPPER ELECTRODE

TUNGSTEN CARBIDE

C / R	300	200	100	50	20	0
3·3	1 / 1/2	1 / 1/2	1 / 1	1 1/4 / 1	1 3/4 / NEG.	1 3/4 / NEG.
5	1 / 1	1 / 1/2	1 1/4 / 1	1 3/4 / 1/2	2 1/2 / 1/2	3 / NEG.
10	2 1/2 / 1/2	5 1/2 / 1/2	4 1/2 / 1	4 / 1	5 1/2 / 1	8 1/2 / NEG.
20	20 / NEG	/ 1/2	8 1/2 / 1/2	11 / 1	9 1/4 / 1	12 1/2 /

MOLY ELECTRODE

C / R	300	200	100	50	20	0
3·3	3/4+ / 1	3/4 / 1	1 / 1/2	1+ / NEG.	1 1/2 + / NEG.	1 1/2 / NEG.
5	1 1/2 / 1/2	1 1/2 / 1/2	1 1/2 + / 1/2	2 / 1/2	2 1/2 / NEG.	2 3/4 / NEG.
10	4 1/4 / 1/2	3 1/2 / 1	3 1/2 / 1/2 +	/	/	/
20	/	/	/	/	/	/

COPPER ELECTRODE

TITANIUM

rates with tungsten carbide are much slower than the other metals tested, as recorded in Table I. The electrode wear was about double that for the other materials tested. The copper electrode gave rather poor results with tungsten carbide since it had a tendency to wear to a point on one side and then proceed to drill a conical-shaped hole. Excellent holes, however, were produced by the molybdenum electrode, especially at R=20 ohms.

E. Drilling of Titanium

Identical tests made with titanium gave results that were very similar to those obtained with the carbon steels, as shown in Table I.

F. Comparison of Drilling of Various Types of Materials

Table I illustrates comparative values of cutting time and electrode disintegration for the various types of materials tested. The head was vibrated at 300 cycles per second. The hole depth in each case was 1/4 inch.

G. Summary

Straight dc gives oversized, rough holes and is unacceptable. The addition of resistor-condenser network does give satisfactory results. The capacity of the condenser should be between 100 and 300 microfarads, and the resistor should be variable over the range of 3 to 25 ohms when surface finish is not the major concern. To obtain the best finish, the capacitance must be decreased by 5 to 15 microfarads.

Although drilling does occur without head vibrations, the head should be vibrated at a rate of 200 cycles per second for best results. When drilling low melting-point materials, copper electrodes wear as well as molybdenum electrodes. On high melting-point materials molybdenum electrodes give better quality holes. Less heating of the workpiece occurs when using the R-C circuit than when using ac because of the smaller arc currents.

IV. METALLURGICAL ASPECT OF ELECTROSPARKED SURFACES

A very detailed metallurgical study of the subsurface material after machining by the electrospark or electroarc process was made, and some very specific clues regarding the mechanism by which the work material is removed were obtained. Several different materials were investigated, but only tool steel and high-speed steel were studied in detail since they exhibit

phase transformations during heating.

A. Carbon Tool Steel

For two reasons, carbon tool steel was selected as the material on which the most exhaustive metallurgical study would be made. First, it can be fully hardened to a value of 67 on the Rockwell "c" scale ($67R_c$) which makes it unmachinable by any of the conventional methods other than grinding. Second, it exhibits numerous phase transformations at specific temperatures and cooling rates, thus making it possible to determine the temperature distribution beneath the surface as illustrated in Figs. 10 and 11. It is not possible to get this kind of information by a similar study of sintered carbide, Stellite-type materials, or some of the stainless steels. However, the same temperature distribution will exist beneath the surface of those materials as is present in the carbon tool steel.

The changes that occur in the microstructure and the approximate temperature at which they occur at various depths beneath the electrosparked surface of tool steel is shown in Fig. 10. Insert 10A shows the microstructure at 500 magnifications of the original or unaffected base material. It consists of white, rounded globules of cementite (iron carbide compound, Fe_3C) in a matrix of gray, untempered martensite. The hardness of this material is 800 to 850KHN (Knoop hardness number) as measured with a Tukon microhardness tester and corresponds to $66R_c$.

About 0.018 inch beneath the surface the base material begins to show evidence of being tempered, that is, reheated and softened. This is indicated by the gray martensite turning darker, as in 10B, and occurs when the steel is reheated to approximately 600°F. At a distance of 0.012 inch from the surface, the martensite is highly tempered, as shown in 10C, which implies that a temperature of 1300°F had existed there. The hardness at this zone is 470KHN ($45R_c$).

At 0.011 inch from the surface there is a transition zone 10D in which both the tempered martensite and new, primary martensite are present. When the tempered martensite is heated in the range of 1350 to 1400°F, it transforms to a different phase or structure that is called austenite, which on rapid cooling changes to untempered martensite that is identical to the original base material. The microhardness in this zone fluctuates between 650 and 890KHN (57 and $67R_c$) depending upon whether the reading is taken near the tempered or the primary martensite.

Insert 10F shows coarser martensite with its characteristic and very pronounced dark needles. Also, there are no white globules of cementite present, as in 10E, which indicates that the temperature at a distance of about 0.008 inch beneath the surface is 1750°F. The hardness at this zone is

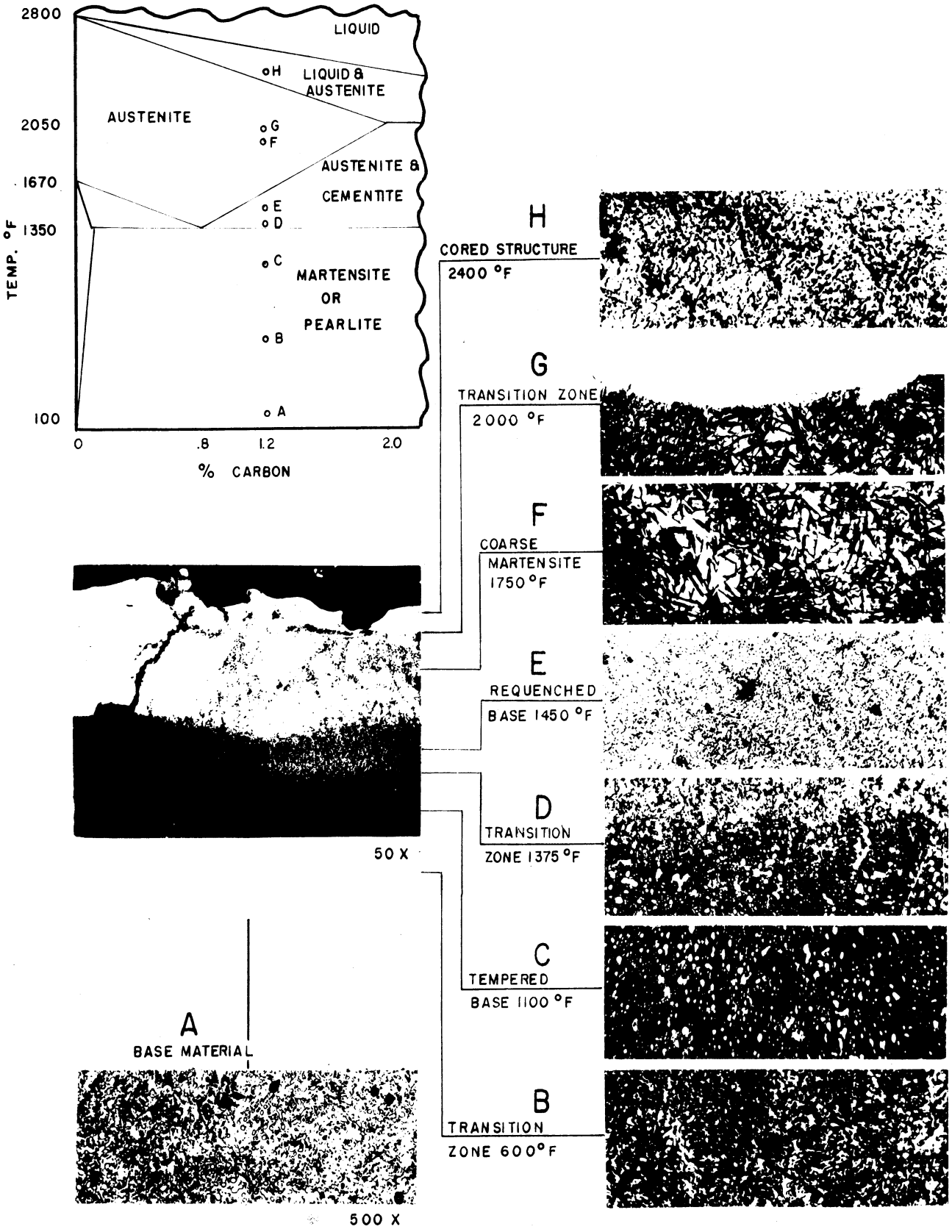

FIGURE 10. PHOTOMICROGRAPHS OF CARBON TOOL STEEL SHOWING CHANGES IN THE MICROSTRUCTURE AT VARIOUS DEPTHS BENEATH AN ELECTRO-SPARKED SURFACE.

the same as the preceding one, 650 to 890KHN.

In zone 10F there are some white areas which on deeper etching show grain-like structures that are pinkish-blue in color and are probably retained austenite or carbides other than cementite.

Insert 10G shows the transition from the coarse martensite to the white-surface material which occurs at a depth of 0.006 inch. This white layer on deeper etching shows a cored, fine-grained structure which is shown more clearly at 1000 magnifications in Fig. 11. The three photographs in Fig. 11 are of the same area of one specimen, the only difference being the focusing of the camera in taking the picture. Figure 11A displays very small grains with a faint dendritic pattern that is present in metals that are cast from the liquid state; 11C illustrates a cored structure with preferential etching. The white, raised regions are probably lower carbon-retained austenite, while the darker material is very fine martensite. The hardness in this region varies between 672 and 985BHN (58 to 69R_c) and consequently it cannot be decarburized as some other investigators claimed without making a microhardness traverse. If the steel had been decarburized, its surface hardness would be about 10 to 20R_c. Thus, it is apparent that the white surface layer is fully hardened and the fact that the hardness is as low as 58 in some places is because of a small amount of austenite being retained due to the very rapid cooling rate. This austenite would transform to the harder martensite if it were given a slight treatment.

When the zones of transformation illustrated in Fig. 10 are plotted, with the apparent temperature as one axis and the distance beneath the surface at which it occurs as the other axis, a curve as illustrated in Fig. 12 is obtained. There is a break in the continuity of the curve between 1300 and 1400°F, which corresponds to the range within which the transformation temperature of the steel lies, and another one between 2000 and 2400°F corresponding to when the metal becomes liquid. Although it would not be correct to extrapolate the curve to the surface it is quite evident that the temperature lies well into the liquid region and probably approaches the vaporization temperature of the steel.

B. High-Speed Steel

The microstructure of the high-speed tool steel (18% tungsten, 4% chromium, 1% vanadium) is shown in Fig. 13. The base material, shown most clearly in the center of 13A, is martensite and carbide of tungsten and chromium, the former being the large gray grains and the latter being the small, round, white grains. This base has a hardness of 985KHN or 69R_c. Nearing the electrosparked surface, the metal is tempered by the heat and the hardness decreases to 770KHN (62R_c) which indicates that a temperature of 1200°F has been reached.

A 1000X B 1000X C 1000X

Fig. 11. Photomicrographs of the White Zone Taken with Different Camera Focus Settings of the Same Area. Figure 11A shows very fine grains with a faint dendritic pattern and a hardness of 58 to 69 Rc; 11B shows how the grains themselves are raised while the grain boundaries are etched deeper; and 11C illustrates the cored structure that is typical of material quenched from the liquid state.

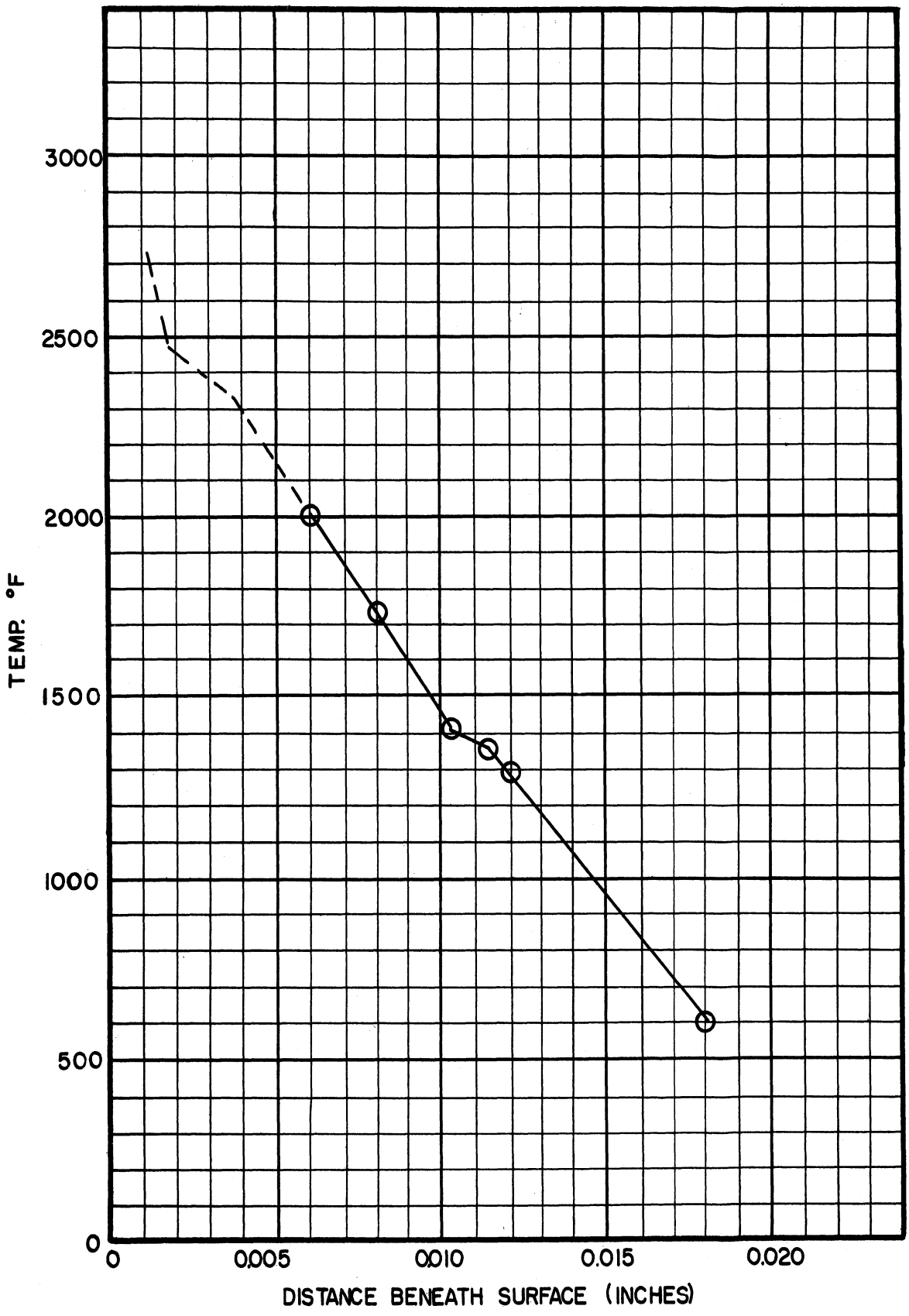

Fig. 12. Approximate Temperatures Beneath the Electro Sparked Surface as indicated from the photomicrographs of carbon tool steel.

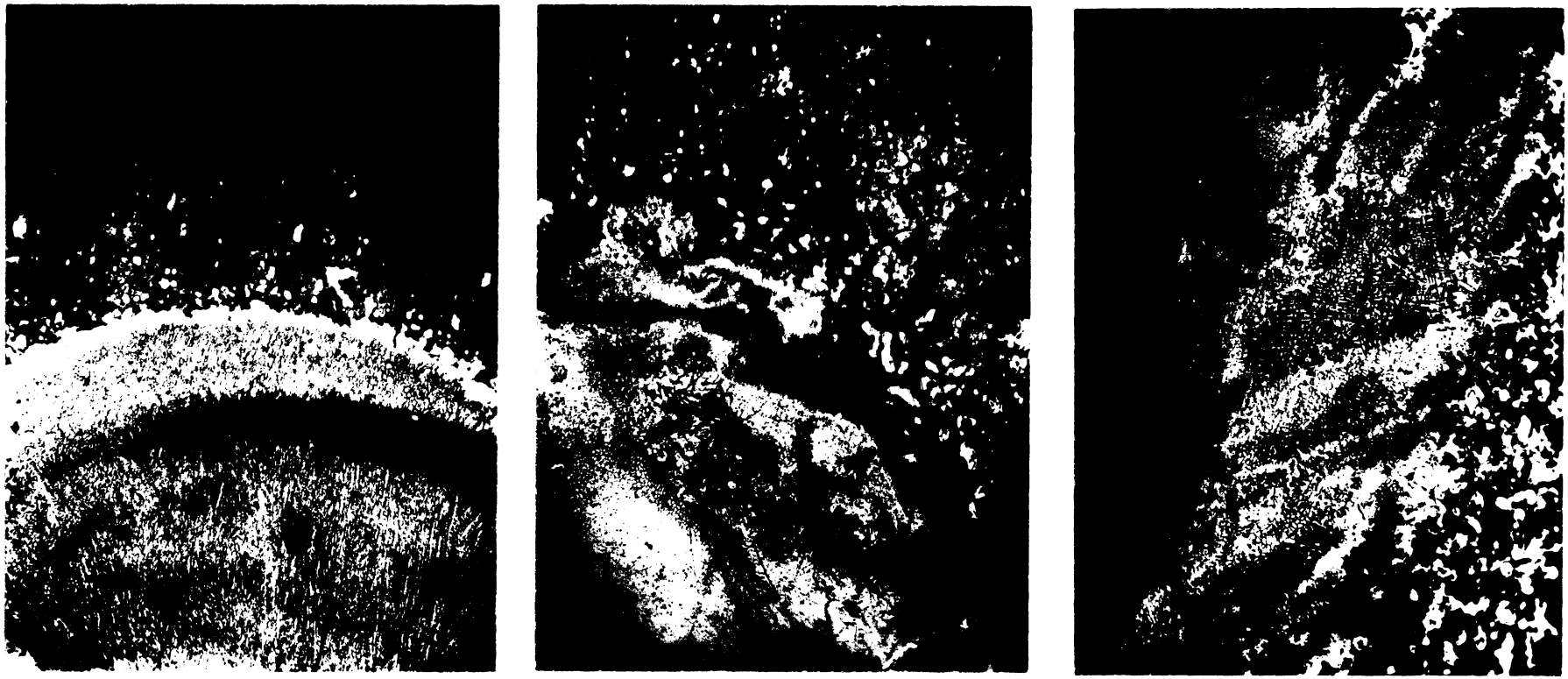

A 400X B 400X C 400X

Fig. 13. Photomicrographs of Subsurface Microstructures in High-Speed Steel After Electrospark Machining. Figure 13A illustrates the martensite base material with dispersed carbide; 13B shows martensite needles in the white zone adjacent to the tempered base; and 13C illustrates the cast, dendritic structure present in the white zone right at the surface.

Nearer the surface is a zone of requenched martensite in which the hardness increases, as expected, to 985KHN. The quenching temperature needed to obtain fully hardened high-speed steel is 2200°F. Figure 13B shows that upon deep etching the martensitic structure in the white zone can be brought out.

Adjacent to the surface the hardness drops to 800KHN, which is due to some retained austenite being present. On deep etching a definite dendritic structure, which is typical of steel when cooled from the liquid state, is exposed and illustrated in Fig. 13C.

C. Low-Carbon Steel

Since the preliminary work on the project was done using low-carbon steel as the work material, a short description of the metallurgical effects upon this material are included here.

The large photomicrograph in Fig. 14 shows at 150X the subsurface material after electrospark machining. It shows a clear line of demarcation between the white zone adjacent to the surface (that is often referred to as "decarburized") and the base material of pearlite (dark grains) and ferrite (light grains). Insert 14A shows this latter material at 500X. The hardness of this pearlite is 300 to 350KHN (26 to 33R_c) and corresponds to pearlite of hot-rolled steel. The ferrite has a hardness of 185 to 210KHN (5 to 10R_c) and is also equivalent of steel in the hot-rolled condition.

In the lower part of the transition zone of insert 14B the ferrite hardness remains the same although the hardness of the now fuzzy-gray grains has increased to 745KHN (66R_c), indicating that they are now no longer pearlite. Consequently, this implies that the temperature of this region was about 1450°F in which case the ferrite would not be changed, but the pearlite on heating would transform to austenite which in turn would transform to the hard martensite on rapid cooling.

Upon prolonged etching several microstructures are discernable in the white zone as illustrated by inserts 14C and 14D. The lower region consists of massive ferrite grains with fine cementite dispersed throughout and was quenched from the solid state, about 1800°F. The hardness of this material is quite uniform throughout at 358 to 409KHN (34 to 39R_c). The upper region consists of fine ferrite with dispersed cementite and was quenched near the liquid temperature, about 2400°F. The hardness of this structure is very uniform, 470 to 488KHN (45 to 47R_c).

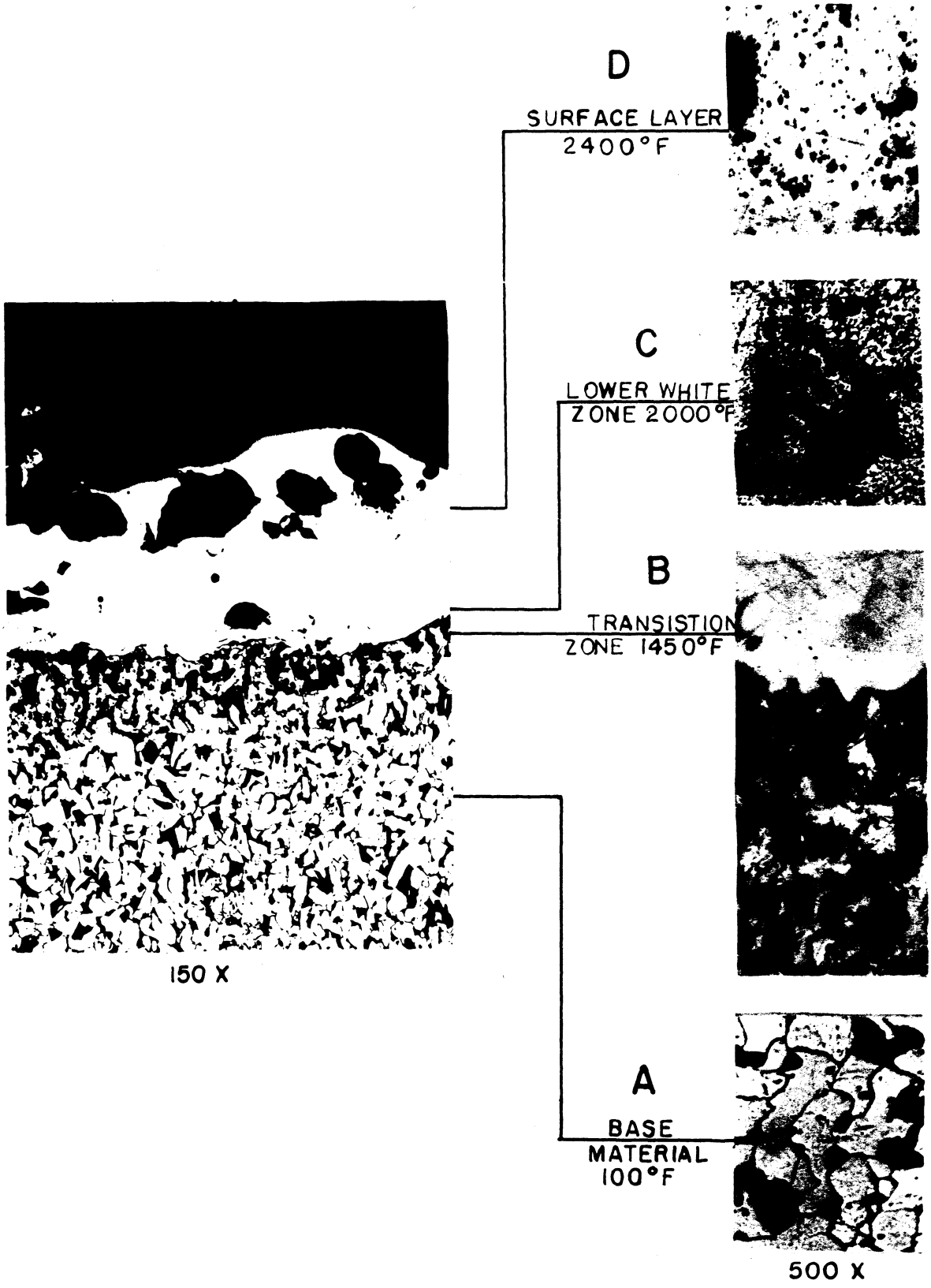

Figure 14. Photomicrographs showing the metallurgical transformation beneath the electro-sparked surface of low carbon steel. The microconstituents are: A, ferrite and pearlite; B, ferrite and martensite; C and D, ferrite and cementite.

D. Stainless Steel and Sintered Carbide

As stated previously, little work was done on these two materials inasmuch as they exhibit no phase transformation upon heating or cooling and, consequently, a metallurgical study can show very little results. The hardness of the base material of the stainless steel in Fig. 15A is about 337KHN (31R_c) and in the white region it is about 470KHN (45R_c), which is probably due to the presence of finer grains and a more highly stressed microstructure. Also, there may be some error in reading the hardness so near the surface of the stainless steel because it is very difficult to polish it without rounding the edges.

Figure 15B shows how the microstructure of the sintered carbide is not affected by temperature. The hardness remained at 1300 to 1500KHN throughout the entire sample. The jagged appearance of the carbide surface is due to the cracking and chipping of the very brittle material. These cracks are caused by the very high stresses which are induced by the steep temperature gradients present beneath the surface.

E. Electrode Build-Up

Under certain drilling conditions described earlier, a build-up was formed around the bottom of the electrode. The size of the build-up gradually increases as the electrode is fed downward, causing a tapered hole that is as much as 1/16 inch in diameter larger at the bottom. This protrusion is attached to the electrode but is not truly welded to it because in removing the electrode from the hole the build-up breaks off and remains in the bottom of the hole as shown in the right of Fig. 16A. This condition became most pronounced with the combination of large resistance and low capacitance which results in low-energy arcs and consequently long drilling times.

Figure 16B shows the build-up material at 500 magnifications after polishing and etching. The diamond-shaped designs are the Knoop indentations. This material is very porous and readily breaks in small pieces which are quite ductile, consequently making it difficult to obtain microhardness values. However, with careful manipulation the hardness of this material ranges from 438 to 703KHN (43 to 59R_c), with the low values being the hardness of the matrix material.

Although this build-up had formed on a molybdenum electrode, a chemical analysis showed there was only 3.5% molybdenum present in the build-up. No crystalline structure was observed in the matrix material even on prolonged etching so it was not possible to ascertain the microstructure of this material. However, on a microscopic scale this build-up appeared to be made of thousands of small spheres randomly bonded together. Since the molybdenum content of them is so low the build-up must have formed by the arc, melting

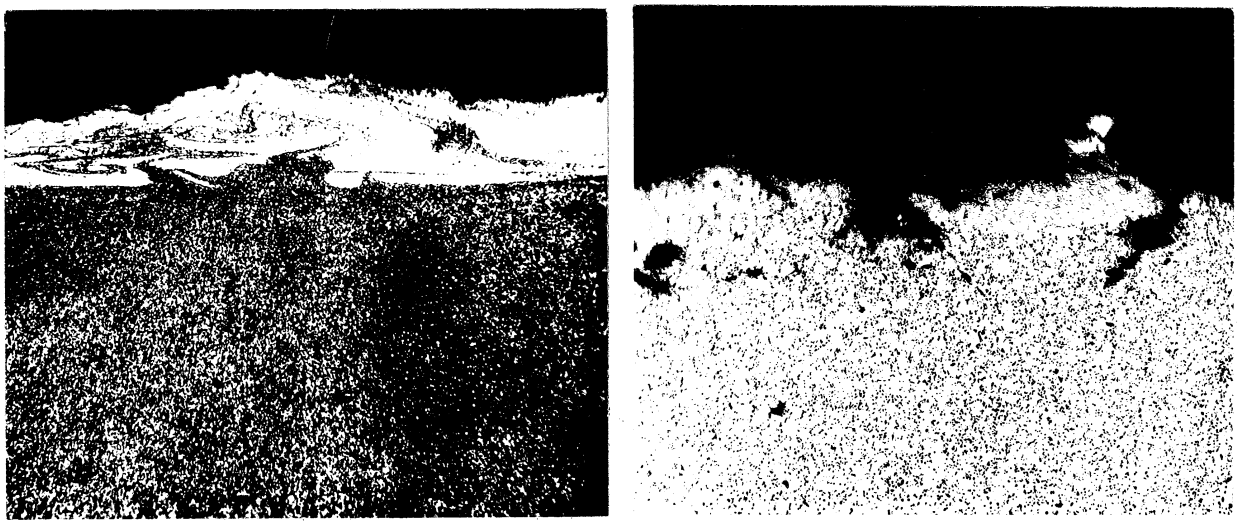

A 500X B 200X

Fig. 15. Photomicrographs of the Subsurface Material of Stainless Steel, (A), and Sintered Carbide (B). The swirled appearance at the surface of the stainless steel indicates that it has been in the liquid state. The jagged appearance of the carbide surface is due to cracking and chipping of the very brittle material caused by very high stresses induced by the steep temperature gradient.

A 1.5X B 500X

Fig. 16. Cross Section of Electrosparked Holes and Electrode Build-Up When Drilling Carbon Tool Steel with a Molybdenum Electrode. Figure 16A shows a cross section and top view of four holes drilled with a head vibration of 180 cycles per second and the following R-C values, starting from the left: 10 ohms and 200 microfarads, 10 ohms and 100 microfarads, 20 ohms and 50 microfarads, 100 ohms and 20 microfarads. Figure 16B shows the polished and etched build-up with the Knoop indentations in it.

small areas of the work material which became spherical and while still partially liquid, attached themselves upon the electrode.

To determine what kind of chips or particles were produced by electrospark machining, some of the cutting fluid was filtered during a drilling operation and a small amount of residue was collected and examined under a microscope. It was found to consist entirely of brown and gray spheres (brown from the copper electrode and gray from the steel work piece) varying in size from less than 0.001 to 0.010 inch in diameter. Some of these are shown in Fig. 17. It is to be noted that all of the chips are very regular spheres, which implies that they had been formed in the liquid state where the surface tension acted to give them their spherical shape. If these chips had been pulled out mechanically or physically by the exertion of very high electrostatic forces, they would be very irregular in shape with jagged and torn surfaces.

F. Mechanism of the Cutting Action

On the basis of the results obtained by the metallographic study of surfaces produced when machining with a Metalmaster disintegrator, it is apparent that the mechanism of metal removal in the electrosparking or electroarcing process is one of thermal means rather than a mechanical rupture of the metal due to the action of large cutting or electrostatic forces. This fact is obvious in consideration of the high temperatures present in the subsurface material, which indicate that temperatures are well above the melting point at the surface. This is further substantiated by the fact that all the chips are spherical rather than irregular in shape as is customary of all chips produced by the exertion of forces upon the material.

In simple terms, the sequence of operations that is responsible for the metal removal may be outlined as follows (see Fig. 17). The vibrating electrode, at the bottom of its downward travel, contacts the work surface at a point corresponding to where projections on the surface of both the work and the electrode coincide. This contact closes the electrical circuit, and for the most efficient metal removal during the time this contact is made, the electrode should be negative and the work positive. This should be done because about 20 percent more of the heat produced at the arc is transferred to the anode than to the cathode.

This electrical contact causes the electric current to flow but, due to the small area of contact, the resistance is high and it raises the temperature at this contact point. This temperature rise is nearly instantaneous and is sufficient to cause the contact projections to melt and vaporize. Also, as the vibrating electrode is raised, the breaking of the electrical contact causes an arc of short duration to form. The high temperature of this arc discharge (about 10,000°F) causes the metal at both ends of the

arc to melt and some to vaporize. The arc is extinguished by breaking the electrical circuit or the discharge of a condenser and the cutting fluid quenches and washes away the particles, which in their molten state have become spherical. In addition to this, the metal removal may be assisted somewhat by the gases that are present in the metal. As the temperature of the subsurface is raised the pressure of the entrapped gas is increased, and when the adjacent metal becomes liquid this compressed gas will cause the liquid metal to be expelled. This phenomenon will, in part, account for the irregular surface produced by the electrosparking process.

The above sequence of operations continues until the job is completed. In brief, this whole operation may be considered as microscopic arc welding in which the liquid metal is washed away by means of a fluid.

G. Holes Drilled by the "Method X" Process

Figure 18A shows the microstructure at 250 magnifications of high-speed tool steel drilled by the "Method X" process. Subsurface material showed the same signs of transformations due to the high temperature as did the specimens drilled with the Metalmaster disintegrator. On this particular specimen the heat-affected zone is somewhat smaller than was present on the previous holes studied, but this is probably due to the operating conditions rather than the process.

The base material consists of martensite and carbide having a hardness of 986KHN ($67R_c$). In the white zone the hardness varied from 880KHN ($67R_c$) adjacent to the tempered base material to 526KHN ($49R_c$) at the surface. A microhardness traverse is included in Fig. 18.

Figure 18B shows the microstructure of a specimen of carbon tool steel drilled by the "Method X" process. The structure varies from a base material of martensite and iron carbide to tempered martensite, then requenched martensite, and finally to a white region that shows some martensite needles on deep etching.

The hardness of the base material is $62R_c$ and it drops through tempering to $54R_c$ adjacent to the requenched martensite zone in which the hardness increases to $68R_c$. The white area has a hardness of $50R_c$ adjacent to the requenched martensite, but it drops to $40R_c$ at the hole surface which is probably due to the rounding off of the surface in polishing. The complete hardness traverse is shown in Fig. 18.

V. ELECTROARC MACHINING OTHER THAN DRILLING

One of the objectives of this first study was to investigate the

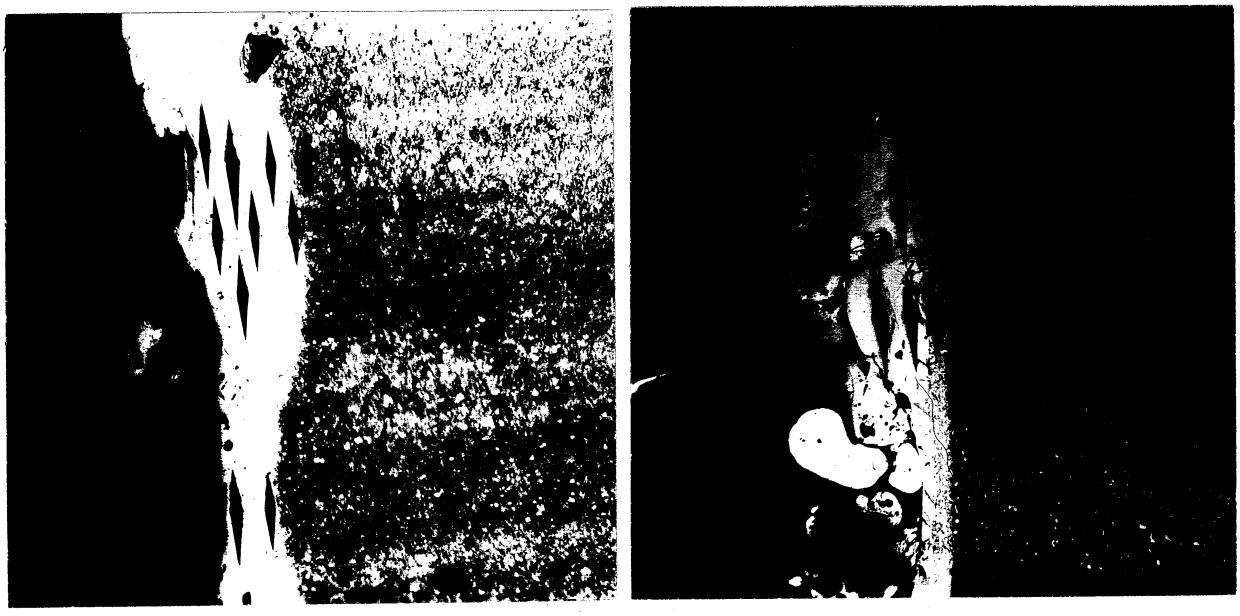

A 250X B 250X

Location	Distance from Hole	KHN	R_c
White Zone	0.0004	526	49
	.0008	644	57
	.0012	769	62
	.0016	806	64
	.0020	847	66
End of White Zone	.0024	880	67
	.0028	885	67
Tempered Base	.0032	950	69
Base Material	.0035	986	69 R_u

Location	Distance from Hole	KHN	R_c
White Zone	0.0004	400	39
White Zone and Some Martensite	.0008	423	
	.0014	526	
Requenched Martensite	.0020	806	
		890	
		940	
Heat-Affected Base Material	.0026	605	
	.0034	703	
	.0039	718	
	.0045	735	
	.0065	740	
Base Material	.0084	760	62

Fig. 18. Photomicrographs of Holes Produced by the "Method X" Process. Figure 18A is 18-4-1 high-speed steel and 18B is carbon tool steel. The diamond-shaped images are the Knoop indentations.

possibilities of using the electrosparking process for machining operations other than the drilling of holes. Consequently, the Metalmaster disintegrator was converted as shown in Fig. 19 so that the external surfaces could be machined. To accomplish this the disintegrator head was disconnected and rotated 90 degrees. A spindle driven by a variable speed motor was attached to the head. A copper disk to serve as the electrode and copper brushes were mounted on this spindle. A vise was attached to feed the work under the disk by means of a second variable-speed motor. The feeding rate was controlled manually with the assistance of an oscilloscope connected across the arc so that it would indicate, by the voltage drop across the arc, whether the feed was too fast or too slow.

In a previous report, 2175-3-T, the feeling was expressed that it might be possible to prevent the cathode disintegration if the discharge could be moved along the surface rapidly. The calculations indicated that the speed should be of the order of 8880 inches per minute or 740 feet per minute. If this were true, it would be very desirable to rotate the disk at this speed since it makes it possible to machine irregular shapes very accurately without having to "true" or "dress" the rotating electrode. Consequently, this was the first thing investigated. The speed of rotation was varied from 25 rpm (55 fpm) to 2000 rpm (4500 fpm) and the cutting time and the disk wear were observed. Contrary to the expectations, there was no speed at which the cathode did not disintegrate or wear as it did in hole drilling. Neither the time to machine a certain area, to cut through a certain specimen, nor the disk wear varied appreciably throughout this wide speed range. In all cases, the flat face of the disk became rounded and the diameter decreased. However, in the speed range from 100 to 500 rpm, the cutting time was slightly lower which was probably due to the fact that the vibration of the spindle was lower in that range. Because of this all further work was done with the disk rotating about 200 rpm.

The disk was used first without serrations on its face but it was found to work more efficiently if slots were cut in its face. This assists the cutting operation by carrying the cutting fluid into the arcing region where it is needed to quench the liquid metal and prevent the cathode from becoming hot.

Since the disk does wear quite rapidly it was felt that external machining by the electrospark process would be most feasible on the "unmachinable" materials. Consequently it was decided to work on sintered carbide and evaluate it on the basis of diamond-ground carbide. One of the main uses of sintered carbide is as a cutting tool material and has to be machined with diamond-impregnated grinding wheels which are expensive, fragile, and scarce.

The surface finish obtained on sintered carbide by electrosparking with several R-C values is shown in Table II. Varying the resistance from 5 to 100 ohms with a capacitance of 200 microfarads had very little effect upon

A

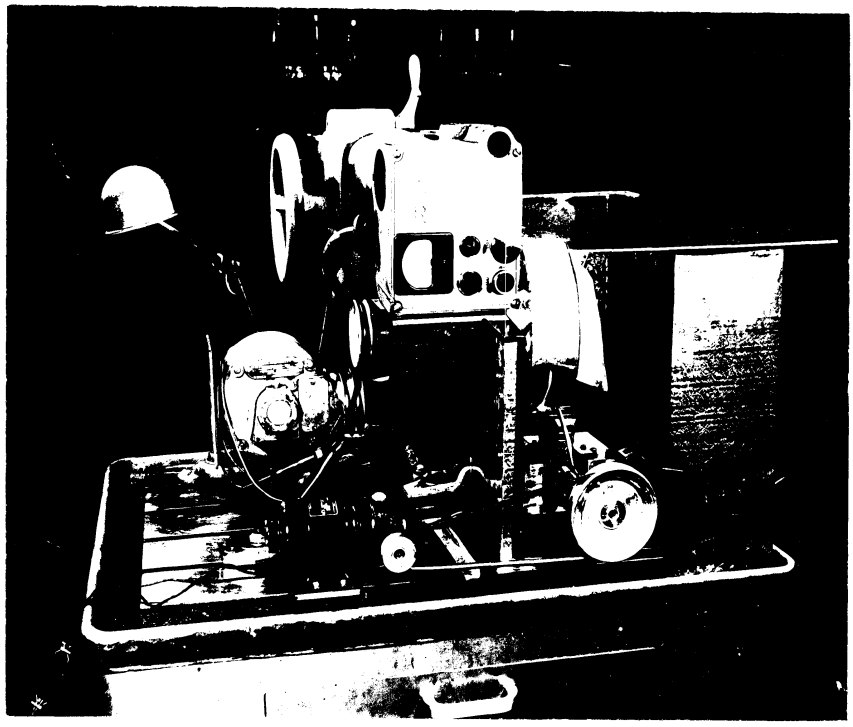

B

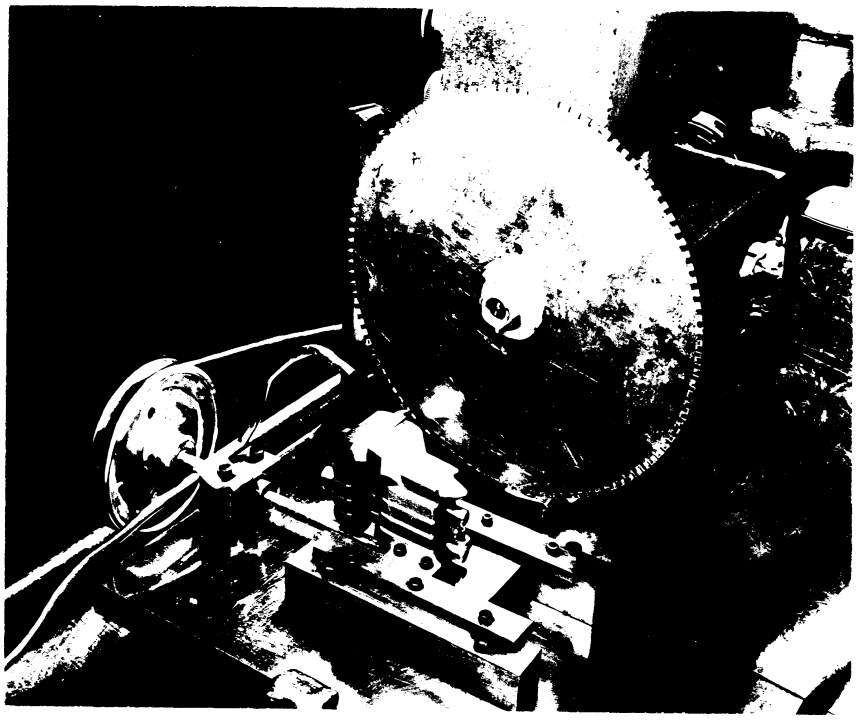

Fig. 19. Photographs of Metalmaster Disintegrator Converted for Tool Grinding. Figure 19A shows a tool being cut by a rotating copper disk that is mounted onto a spindle attached to the disintegrator head. 19B shows a closeup of the cutting disk and the feeding mechanism that moves the tool under the disk. The copper tool at the left directs the cutting fluid into the zone of cutting.

the surface finish. However, by using low values of capacitance the surface finish was improved considerably so that the readings of 60 microinches rms were obtained. With a heavier, more rigid spindle having less vibrations much lower values could probably be obtained with the low capacitance.

TABLE II

EFFECT OF R-C VALUES ON SURFACE FINISH
OF ELECTROSPARKED CARBIDE TOOLS

Sharpening Conditions: diameter of disk = 9"
width of disk = 1/4"
Periphery of disk was serrated: rpm = 200

No.	R (ohm)	C (μf)	Surface Finish (μin. rms)
1	5	200	120-160
2	10	200	80-170
3	20	200	140-160
4	50	200	120-150
5	100	200	90-150
6	100	15	60-70
7	100	5	70-90

VI. MACHINING WITH ELECTROSPARKED TOOLS

To evaluate the ability of carbide tools, sharpened by means of the electrosparked process, to cut satisfactorily with a reasonable tool life, it was decided to use single-point tools and run turning tests on an engine lathe. Consequently, 3/4-inch square carbide-tipped tools were used and the work was done on a 14-inch American Pacemaker lathe equipped with a 15 horsepower variable speed drive. For the work material, 4-inch round SAE 1045 steel and 8-inch-diameter cast iron cylinders 30 inches long were used.

The first series of tests was run to determine the reliability of electrosparked and diamond-ground carbide tools, that is, to see how much variation in the performance there would be between several tools sharpened under identical conditions.

The performance of seven electrosparked tools and seven diamond-ground tools are shown in Table III.

The performance was determined by measuring both the flank wear and the maximum wear which occurred at the nose radius after cutting for 0.9 min-

ute. From this table it is obvious that the reliability of the electrosparked tools is as good or better than that of the diamond-ground tools. Both the average values of the tool wear and the range of values between the seven tools were very much alike in both cases. The average of the maximum wear of the electrosparked tools was 0.024 inch with a range of 0.014 inch between the best and the worst tool. For the diamond-ground tools the average of the maximum wear was 0.028 inch with a range of 0.014 inch.

TABLE III

RELIABILITY OF ELECTROSPARKED AND DIAMOND-GROUND CARBIDE TOOLS

No.	Electrosparked (R=100 ohms, C=200 μf)			Diamond-Ground		
	Max Wear	Flank Wear	Surface Finish (rms)	Max Wear	Flank Wear	Surface Finish (rms)
1	.026	.0075	60-120	.030	.005	4-5
2	.028	.0075	60-120	.033	.006	4-5
3	.022	.0095	60-120	.026	.0065	4-5
4	.023	.0095	60-120	.029	.0065	4-5
5	.016	.0090	60-120	.026	.0035	4-5
6	.023	.0095	60-120	.019	.0030	4-5
7	.030	.0075	60-120	.031	.0035	4-5
Ave	.024	.0086		.028	.005	
Range	.014	.002		.014	.003	

Work Material: SAE 1045	Cutting Speed: 680 fpm
Tool Material: Carbide	Depth of Cut: .100 fpm
Tool Shape: 0°, 0°, 7°, 7°, 7°, 0°, 1/64"	Feed: .012 ipr
Coolant: None	Cutting Time: 0.9 min

Table IV shows the effect of various resistance and capacitance values on tool wear with diamond-ground tools as a basis for comparison. In the four separate groups of tests shown here in which sixty tools were tested, there is no significant trend indicated when no cutting fluid is used although the resistance was varied from 5 to 200 ohms and the capacitance was varied from 200 to 5 microfarads. However, the greatest wear occurred on the tools sharpened with the high capacitance.

In the last group of tests in which a water soluble cutting oil was used, the wear did show a tendency to decrease as the capacitance was reduced

from 200 to 5 microfarads with the resistance of 100 ohms. This trend seems quite reasonable since it conforms to the improvement in the surface of the tool face with the low-capacitance values.

TABLE IV

EFFECT OF R-C VALUES ON TOOL WEAR

Work Material: SAE 1045 — Cutting Speed: 680 fpm
Tool Material: Carbide — Depth of Cut: 0.100 in.
Tool Shape: 0°, 0°, 7°, 7°, 7°, 0°, 1/64" — Feed: 0.012 ipr

Tool	R(ohm)	C(μf)	Cutting Time (min)	Maximum* Wear (in.)	Flank* Wear (in.)
			Without Cutting Fluid		
DG**	-	-	0.7	.023	.005
ES**	5	200	0.7	.055	-
ES	20	200	0.7	.035	.008
ES	100	200	0.7	.033	.013
ES	200	200	0.7	.033	.013
ES	100	15	0.7	.030	.006
DG	-	-	0.9	.028	.005
ES	50	200	0.9	.058	.012
ES	100	200	0.9	.024	.009
DG	-	-	1.0	.030	.004
ES	5	200	1.0	.030	.006
ES	100	200	1.0	.028	.005
ES	100	15	1.0	.036	.005
ES	100	5	1.0	.038	.005
			With Cutting Fluid - Water Soluble Oil (20:1)		
DG	-	-		.029	.0042
ES	5	200		.028	.0070
ES	100	200		.023	.005
ES	100	15		.022	.005
ES	100	10		.021	.0065
ES	100	5		.027	.004

* Average value of three or more tools.

** DG = Diamond-ground. ES = Electrosparked.

Figures 20 and 21 show the results of machining tests on a lathe when cutting cast iron with both diamond-ground and electrosparked tools without the use of a cutting fluid. During the 8 minutes of cutting in which 8 cubic inches of metal per tool were removed, the maximum tool wear on the radius tended to be slightly greater on the electrosparked tools. However, as seen in Fig. 20, the flank wear was very nearly alike for both the electrosparked and diamond-ground tools.

Figure 22 shows results of a series of turning tests on SAE 1045 steel when cutting with sufficient mineral oil. For this series of tests a lower cutting speed was used in order to duplicate more closely commercial practice where a tool life of 30 minutes to several hours is more common than the shorter tool lives used in the laboratory. When using carbide-tipped tools it is desirable to consider a tool as having failed or become dull when the flank wear reaches 0.030 inch.

The tool-wear progression depicted in Fig. 22 is characteristic of tool-life curves obtained when cutting with sintered carbide tools at this speed. These characteristic features of a tool-wear curve show a rapid increase in the flank wear until a value of approximately 0.010 inch is reached at which point the curve levels off and the wear increases at a slower rate. In this figure it is apparent that the wear rate is very similar for both the diamond-ground and the electrosparked tools. Although the initial wear on the electrosparked tool was slightly greater, the wear after 39 minutes of cutting was less than that of the diamond-ground tool, the actual values being 0.017 inch for the electrosparked tool and 0.017 inch for the diamond-ground tool. In view of the fact that only one tool under either of these conditions was tested, it would be more diplomatic, when comparing these two methods of sharpening carbide tools, to state that the electrosparked tools perform as well as similar tools that are diamond-ground to a surface finish of 3 to 4 microinches.

There are probably three characteristics of the electrosparked surface of a cutting tool with a roughness of 50 to 100 microinches that permit it to perform as well or better than a much smoother diamond-ground tool when using a cutting fluid. First, since the surface consists of minute, overlapping craters which are able to retain the cutting fluid, it is reasonable to assume that the chip-tool contact area will be much better lubricated and cause less wear. Secondly, since the surface layer did consist of some liquid metal which, because of the surface tension of the liquid, resulted in a smooth, glasslike surface on the previously mentioned craters. This glazed surface would have a very low coefficient of friction and cause the wear to be reduced. Lastly, due to the high temperature in the arc many of the gases present and formed come in contact with the liquid surface material and form oxides or nitrides so small that they are not seen in the "white zone". This surface would also have a lower coefficient of friction than the clean metal and likewise result in less tool wear.

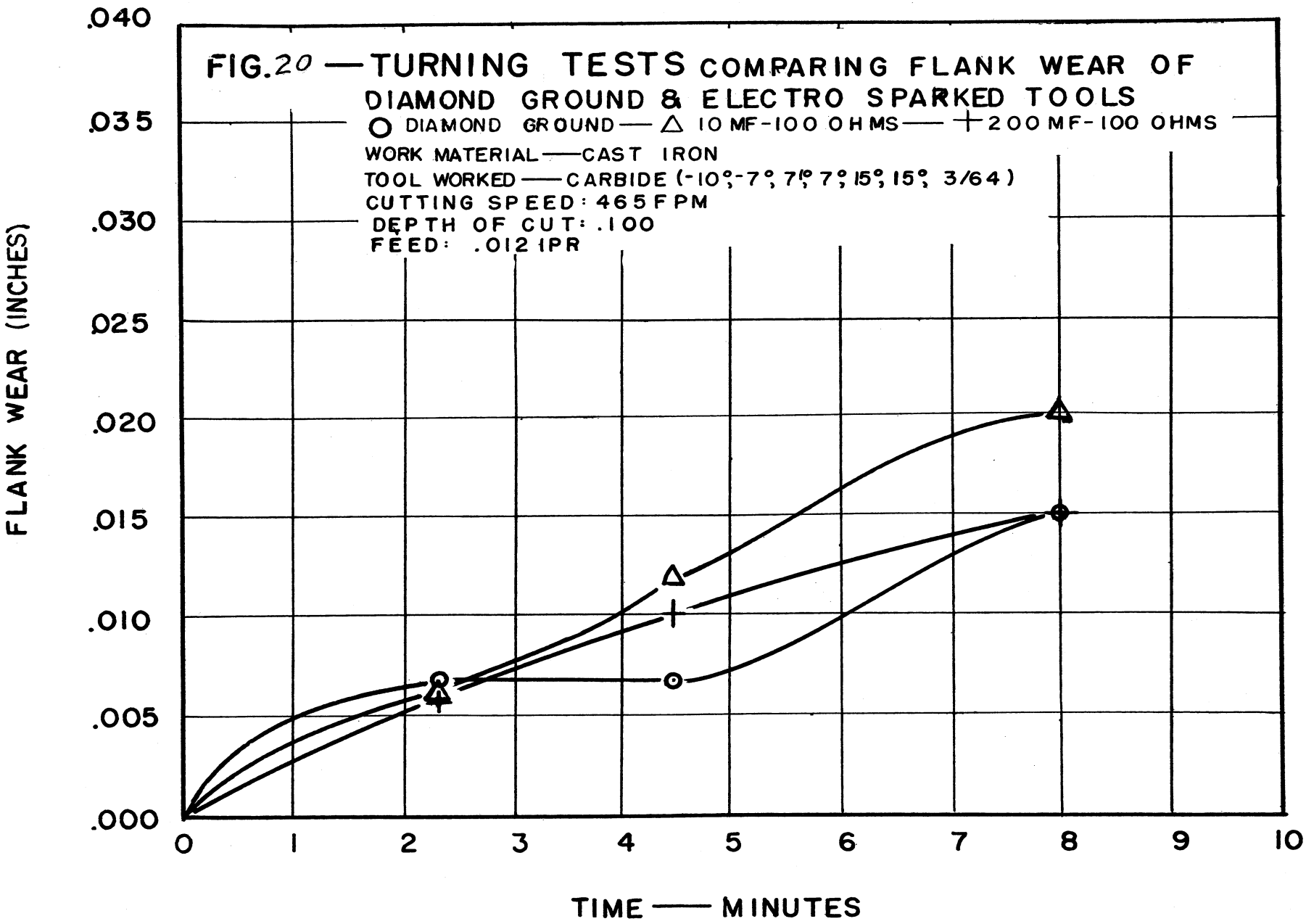
FIG. 20 — TURNING TESTS COMPARING FLANK WEAR OF DIAMOND GROUND & ELECTRO SPARKED TOOLS
O DIAMOND GROUND — △ 10 MF-100 OHMS — + 200 MF-100 OHMS
WORK MATERIAL — CAST IRON
TOOL WORKED — CARBIDE (-10°, -7°, 7°, 7°, 15°, 15°, 3/64)
CUTTING SPEED: 465 FPM
DEPTH OF CUT: .100
FEED: .012 IPR
FLANK WEAR (INCHES)
.040
.035
.030
.025
.020
.015
.010
.005
.000
0
1
2
3
4
5
6
7
8
9
10
TIME — MINUTES

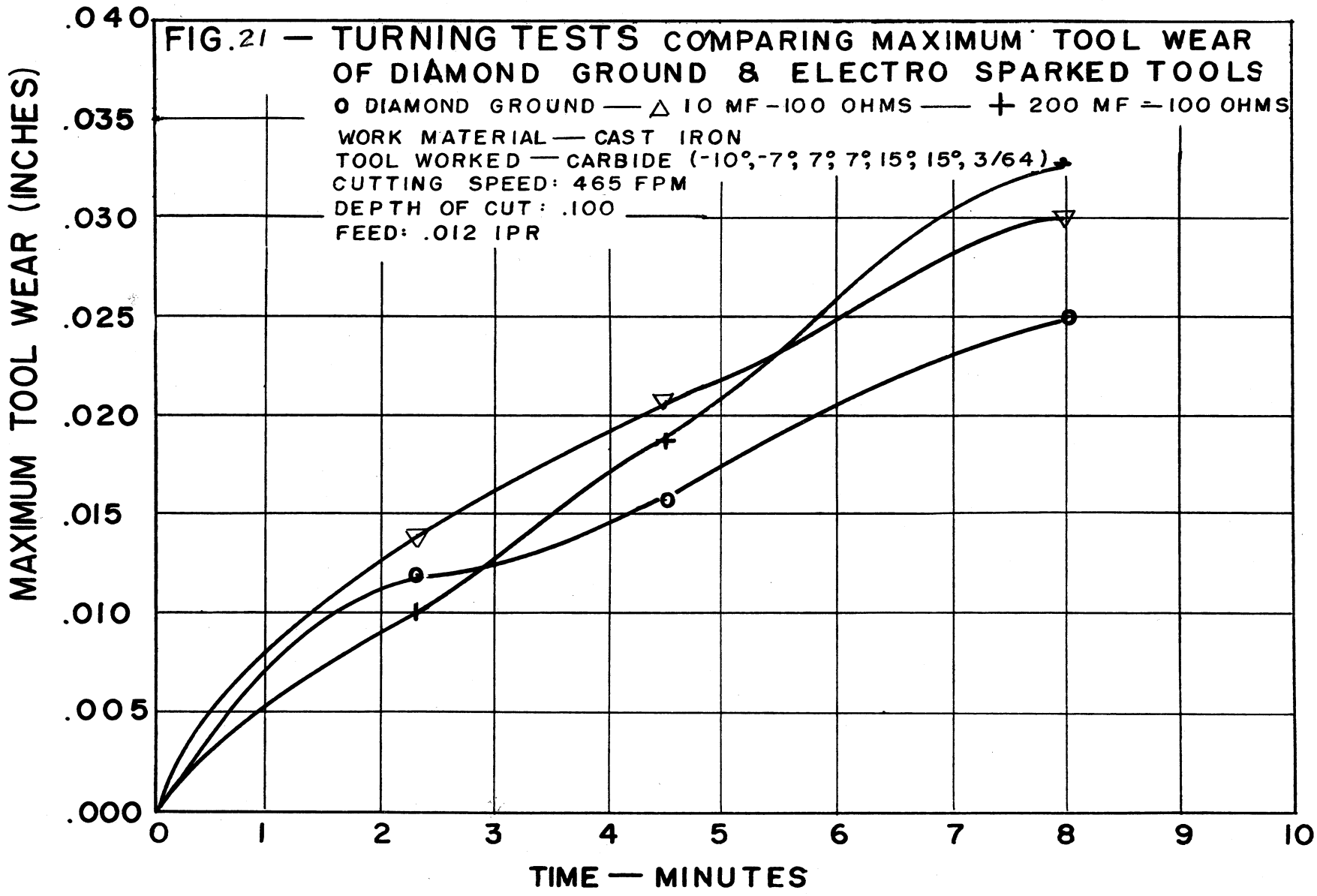
FIG. 21 — TURNING TESTS COMPARING MAXIMUM TOOL WEAR OF DIAMOND GROUND & ELECTRO SPARKED TOOLS
O DIAMOND GROUND — △ 10 MF - 100 OHMS — + 200 MF - 100 OHMS
WORK MATERIAL — CAST IRON
TOOL WORKED — CARBIDE (-10°, -7°, 7°, 7°, 15°, 15°, 3/64)
CUTTING SPEED: 465 FPM
DEPTH OF CUT: .100
FEED: .012 IPR
MAXIMUM TOOL WEAR (INCHES)
.040
.035
.030
.025
.020
.015
.010
.005
.000
0
1
2
3
4
5
6
7
8
9
10
TIME — MINUTES

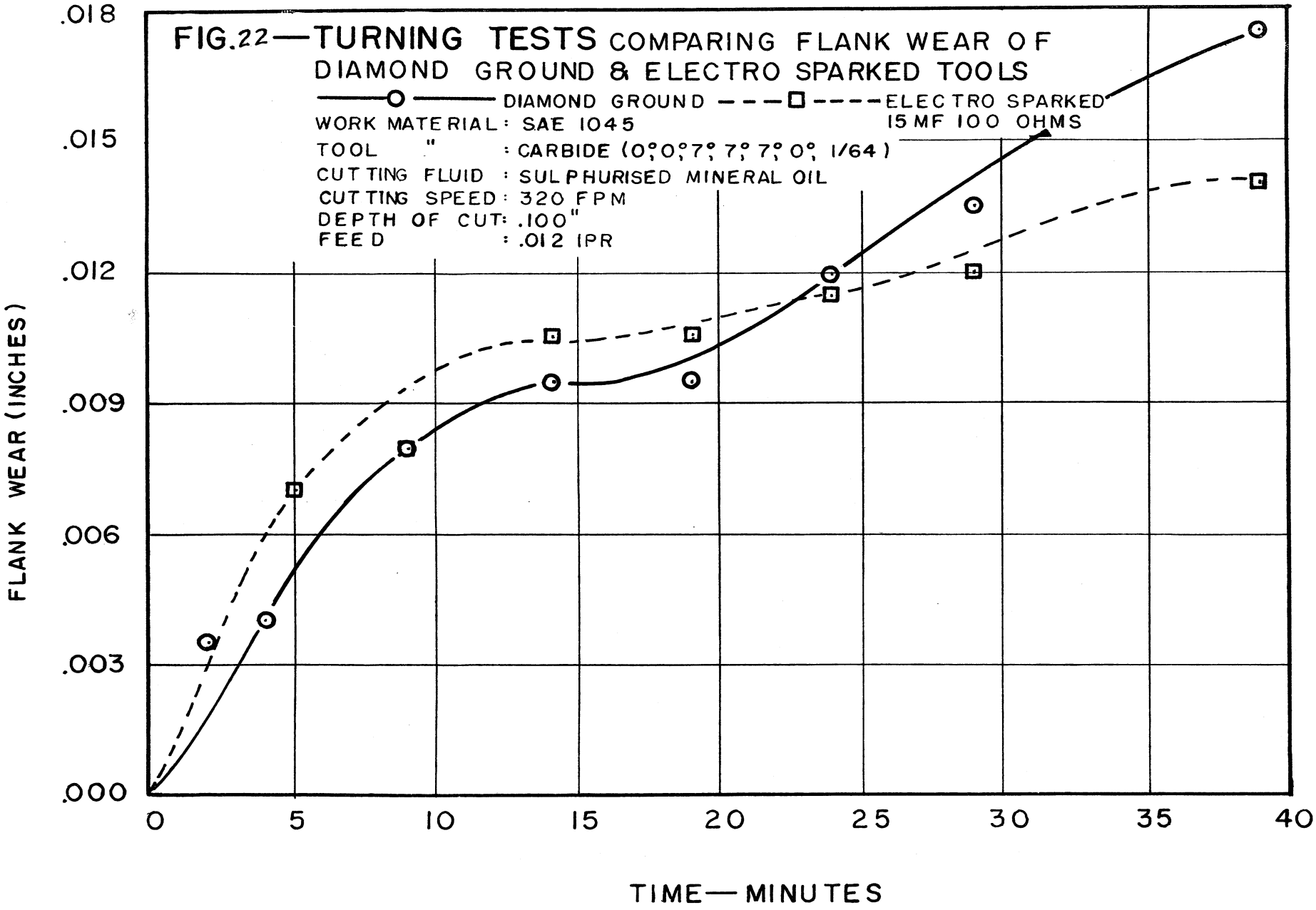
FIG. 22 — TURNING TESTS COMPARING FLANK WEAR OF DIAMOND GROUND & ELECTRO SPARKED TOOLS
DIAMOND GROUND
ELECTRO SPARKED 15 MF 100 OHMS
WORK MATERIAL : SAE 1045
TOOL " : CARBIDE (0°, 0°, 7°, 7°, 7°, 0°, 1/64)
CUTTING FLUID : SULPHURISED MINERAL OIL
CUTTING SPEED : 320 FPM
DEPTH OF CUT : .100"
FEED : .012 IPR
FLANK WEAR (INCHES)
.018
.015
.012
.009
.006
.003
.000
0
5
10
15
20
25
30
35
40
TIME — MINUTES

VII. RESIDUAL STRESSES IN ELECTROSPARKED SURFACES

The final objective of this project was to investigate the electrosparked surface and the subsurface material to determine whether any severe stresses were imparted into the work material. It was not intended to make a detailed study of the distribution of the stresses beneath the surface but merely to ascertain whether the stresses were as large as those induced by other machining operations.

All metal cutting operations induce residual stresses in the surface of the work material, some being compressive and others tensile. In cutting unhardened material with shaped cutting tools the surface layer undergoes severe distortion or work hardening, as evidenced by the numerous studies made showing the increase in the microhardness of the machined surface. The shearing of the metal to form the chip and the friction of the sliding chip on the tool face generate a considerable amount of heat with a resulting rise in temperature. However, when cutting the unhardened material with sharp tools, most of the heat goes out with the chips and the temperature of the work surface remains low. The stresses remaining in this material after machining are generally referred to as mechanically induced and are usually of a compressive nature.

In machining the hard materials such as hardened steel, cast nonferrous metals, and sintered carbides, grinding with abrasive wheels must be resorted to. From a metal-removal point of view this is a very inefficient operation that must be performed at a high speed which causes sufficiently high temperatures on the surface of the work to induce stresses of a thermal origin that are usually of a tensile nature. Although tensile stresses are more objectionable than compressive ones, the most critical situation in dealing with very hard materials is when there is a very steep stress gradient at the surface, since this sets up very large shear stresses parallel to the work surface with resulting chipping or flaking.

In the grinding of hardened steel it has been shown by Letner* and substantiated by others, including some work at the University of Michigan, that the tensile stress at the surface of the ground part could be as great as the tensile strength of the material. But even worse is the fact that the stresses at a distance of only 0.001 inch or so beneath the surface would reverse in sign, that is, be in compression.

To evaluate the stresses induced by electrosparking, specimens of

*Letner, H. R. and Snyder, H. J., "Grinding and Lapping Stresses in Manganese Oil-Hardening Tool Steel," Trans, ASME, July, 1953.

steel and titanium were made 1/8 inch square and 2-1/2 inches long. The titanium was made stress-free by annealing, and the hardened tool steel was made stress-free by removing the surface layer to a depth of 0.015 inch by very light grinding.

The method of determining the residual stress in this study is based on the principle that when a layer of stressed material is removed from a specimen that has a nonhomogeneous stress pattern, the shape of the specimen will change. In the case of a simple beam this change in shape will be a change in the curvature of the beam due to the relief of the remaining portion of the specimen from the stresses contained in the removed layer. If this change in curvature is measured accurately it is possible to calculate the stresses that were in the layer that was removed. Consequently, to determine the residual stresses present in a specimen it is necessary merely to measure the curvative of the specimen as successive layers are removed. The process of removing the thin layers must be such that it does not induce any significant stresses into the specimen. This is best done by etching the stressed surface with an appropriate acid.

The fixture for measuring the curvative is shown in Fig. 23. The deviation of the specimen from the line passing through the two supporting points P was determined by means of a dial indicator reading in 10/1000 of an inch. Readings were taken at the five points indicated in the sketch. The curvature, which is the reciprocal of the radius, is then obtained from the expression $C = \frac{8h}{\ell^2}$ where h is the arc height and ℓ is the distance between centers of the locating pins. This is based on the commonly accepted assumption that the curvature is circular.

These measured curvatures are then plotted as a function of the amount of metal etched away as shown in Fig. 24. The significance of this type of plot is that it shows the qualitative nature of the stress distribution beneath the machined surface without going through a lot of mathematical calculations. If the stresses in a specimen are low and uniformly distributed throughout, the curvature of the specimen will not vary appreciably when layers are removed by etching. The reason etching by means of a dilute nitric acid is used to remove the thin layers is, of course, because no new stresses are induced by this metal-removal technique. From Fig. 24, it is apparent that the stresses induced in the titanium specimen by electrosparking with a large capacitance in the circuit are quite large because the curvature changes from 0.0025 to 0.0130 inch. These stresses are tensile since the curvature values are positive. Also, since the curve falls off more or less uniformly as the layers are etched away, the stresses will also decrease somewhat uniformly beneath the surface.

In general, these curvature curves do not exhibit the reversal in slope that is usually found in specimens ground with an abrasive wheel. This reversal in slope is very detrimental in that it indicates a reversal in sign

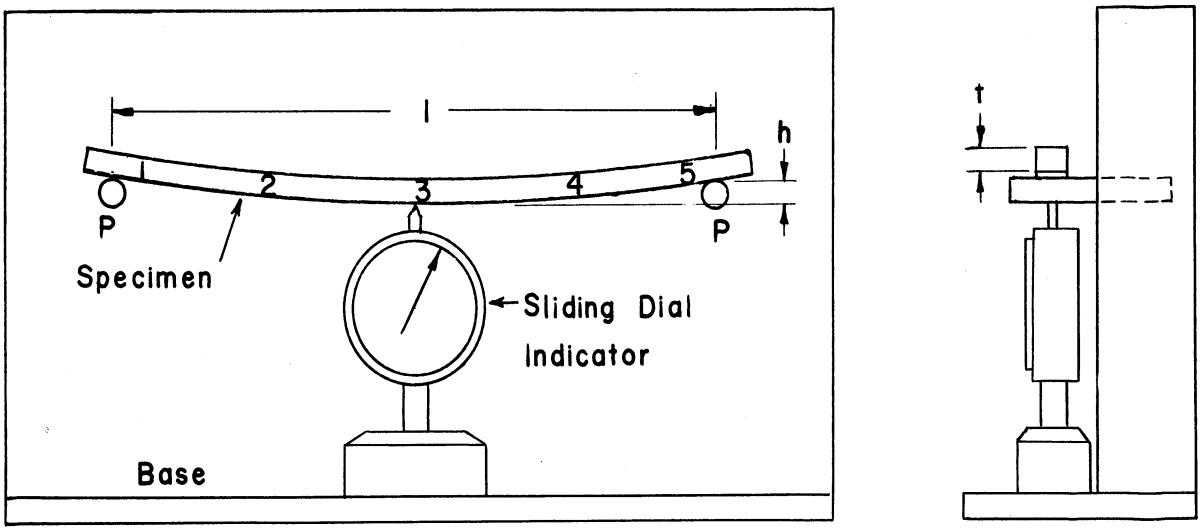

FIGURE 23. FIXTURE FOR MEASURING THE CURVATURE OF A SIMPLY - SUPPORTED BEAM

The specimen, with the electro-sparked surface up, is placed on the two supporting dowel pins 'P'. The dial indicator is moved under positions 1 to 5 and the readings are recorded to the nearest 0.0001". The curvature, which is the reciprocal of the radius, is calculated from the expression $C = 8h/l^2$. When the specimen is concave downwards, as shown in the sketch, the curvature is considered positive in order that the calculated stresses will be of the proper sign.

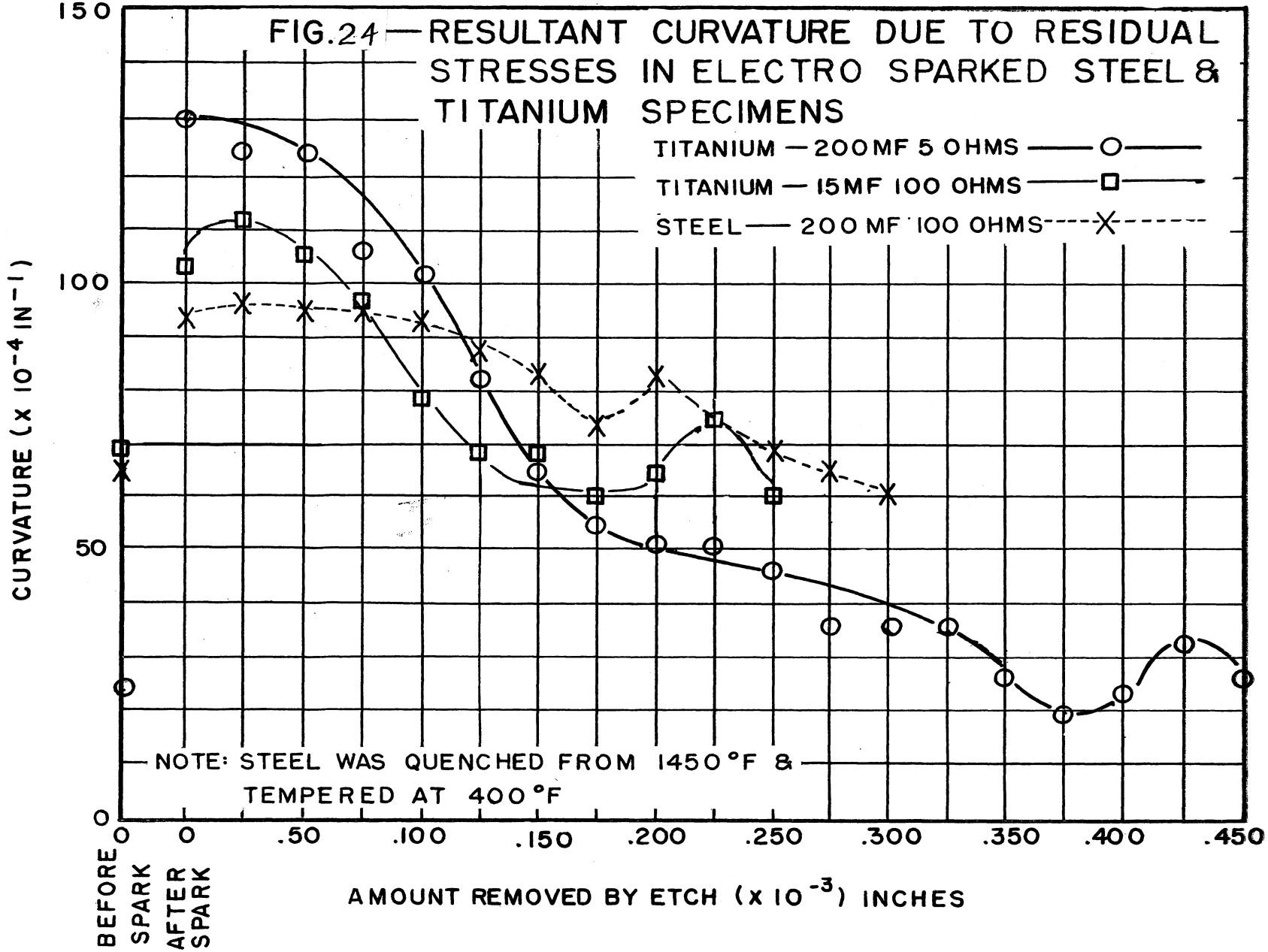
FIG. 24 — RESULTANT CURVATURE DUE TO RESIDUAL STRESSES IN ELECTRO SPARKED STEEL & TITANIUM SPECIMENS
TITANIUM — 200 MF 5 OHMS
TITANIUM — 15 MF 100 OHMS
STEEL — 200 MF 100 OHMS
NOTE: STEEL WAS QUENCHED FROM 1450 °F & TEMPERED AT 400 °F
CURVATURE (x 10⁻⁴ IN⁻¹)
150
100
50
0
0
0
.50
.100
.150
.200
.250
.300
.350
.400
.450
BEFORE SPARK
AFTER SPARK
AMOUNT REMOVED BY ETCH (x 10⁻³) INCHES

of the stresses, that is, compressive stresses in one layer and tensile stresses in an adjacent layer. This condition sets up very large shear stresses parallel to the surface and causes spalling or flaking of the surface.

As seen in Fig. 24, the results shown for the specimen electrosparked with the lower capacitance are quite encouraging since the curvature increased from 0.07 to only 0.10 inch. The tool-steel specimen showed an even less severe stress distribution.

In order to obtain a quantitative idea of the nature of the stresses, calculations were made on the titanium specimen that was electrosparked with the low (15 μf) capacitance. Since the specimen is long in comparison to its width, the calculations were made by means of the simplified expression:*

$$S = \frac{Et^2}{6}\frac{dc}{dt} - \frac{Et}{2}(Co - C) - \frac{1}{t}\int_{t}^{to} Sdt \quad ,$$

which considers stresses in the longitudinal direction only. The value of the last term in this expression is small and can be neglected. The most sensitive term in the above relationship is dc/dt, that is, the change in curvature as the layers are etched away. These calculations were made and the residual stress distribution in the original specimen is shown in Fig. 25. Of course, it must be kept in mind that this was only a survey into residual stresses and the results are in no way conclusive.

Since it appears that one of the most promising fields of application of this process is in the machining of the very abrasive and hard materials that are coming into widespread use in the gas turbine and aviation industries where very thin parts that are subjected to relatively high stresses are used, it would be very important to understand more about the nature of the residual stresses induced by electrosparking. The nature of the residual stresses beneath any machined surface is the information that the designers and process engineers are requiring more and more in all their work. Consequently, it is felt that the nature and cause of these residual stresses should be the subject of any future studies made on this machining process.

---

*Richards, D.G., "Mechanically Induced Residual Stresses," Experimental Stress Analysis, III, No. 1, 40.

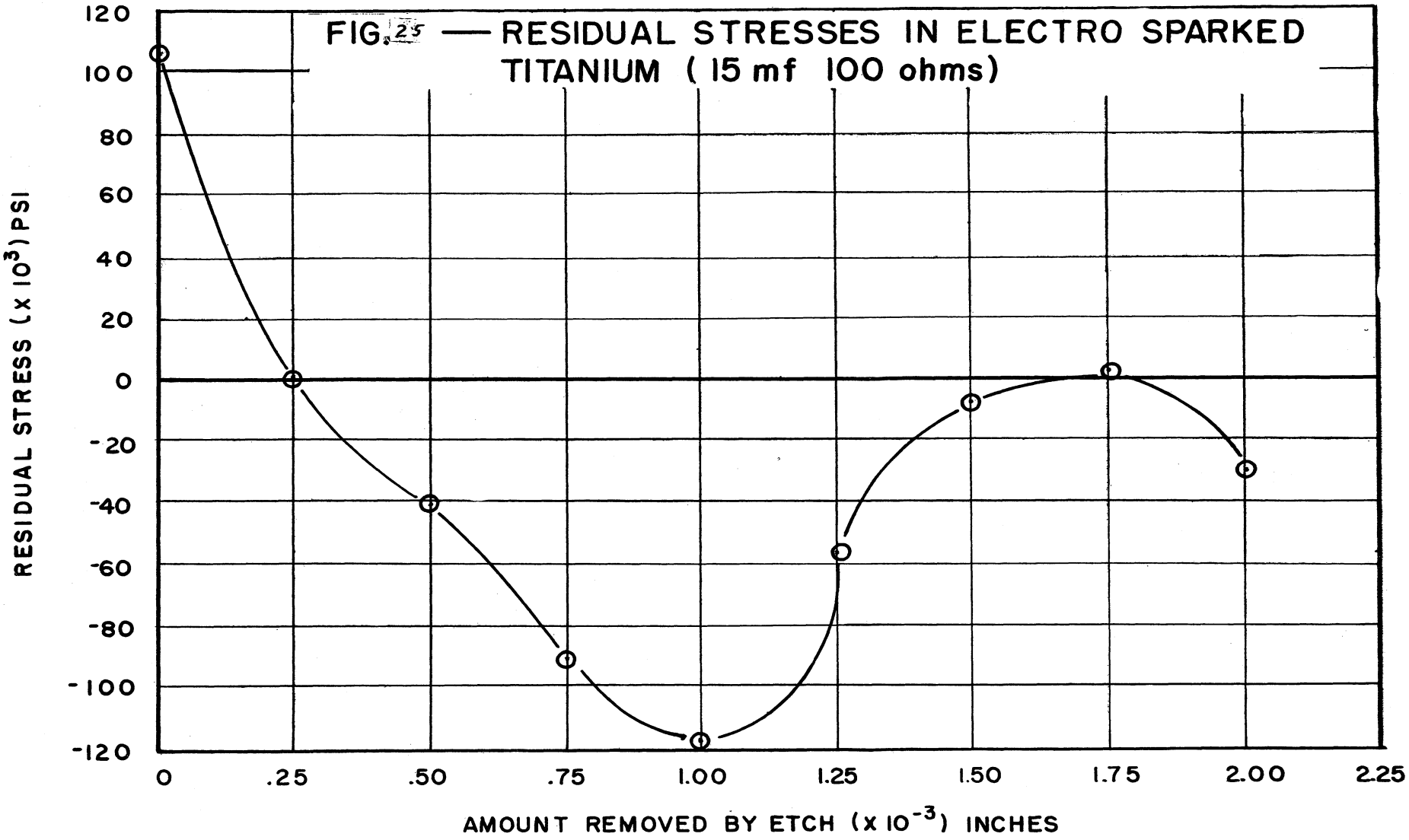
FIG. 25 — RESIDUAL STRESSES IN ELECTRO SPARKED TITANIUM (15 mf 100 ohms)
RESIDUAL STRESS (x 10³) PSI
120
100
80
60
40
20
0
-20
-40
-60
-80
-100
-120
0
.25
.50
.75
1.00
1.25
1.50
1.75
2.00
2.25
AMOUNT REMOVED BY ETCH (x 10⁻³) INCHES